Research on experimental models of neurodegenerative disorders and radiation-induced brain injury

PhD Thesis

IMOLA PLANGÁR

Supervisor:
Dr. Péter Klivényi

Department of Neurology
Faculty of Medicine
Albert Szent-Györgyi Clinical Centre
University of Szeged

Szeged

2014

Original publications directly related to the PhD thesis

I. **Plangár I**, Zádori D, Szalárdy L, Vécsei L, Klivényi P. (2013) Assessment of the role of multidrug resistance-associated proteins in MPTP neurotoxicity in mice. Ideggyogy Sz 66: 407–414.
IF: 0.348

II. Nagy K, **Plangár I,** Tuka B, Gellért L, Varga D, Demeter I, Farkas T, Kis Z, Marosi M, Zádori D, Klivényi P, Fülöp F, Szatmári I, Vécsei L, Toldi J. (2011) Synthesis and biological effects of some kynurenic acid analogs. Bioorg Med Chem 19:7590–7596.

IF: 2.921

III. Kalincsák J, Farkas R, Kovács P, Aradi M, Bellyei Sz, Weiczner R, Sebestyén Zs, **Plangár I**, Hideghéty K. (2013) Single dose irradiation of defined region of rat brain with stereotactic BrainLab system. Ideggyogy Sz (ahead of print)
IF: 0.348

IV. Hideghéty K, **Plangár I,** Mán I, Fekete G, Nagy Z, Volford G, Tőkés T, Szabó E, Szabó Z, Brinyiczki K, Mózes P, Németh I. (2013) Development of a small-animal focal brain irradiation model to study radiation injury and radiation-injury modifiers. Int J Radiat Biol 89:645–655.

IF: 1.895

V. **Plangár I**, Szabó ER, Tőkés T, Mán I, Brinyiczki K, Fekete G, Németh IB, Ghyczy M, Boros M, Hideghéty K. (2013) Radio-neuroprotective effect of L-alpha-glycerylphosphorylcholine (GPC) in an experimental rat model. J Neurooncol (under review)

Total impact factor: **5.512**

Publications not directly related to the thesis

I. Tőkés T, Varga G, Garab D, Nagy Z, Fekete G, Tuboly E, **Plangár I**, Mán I, Szabó RE, Szabó Z, Volford G, Ghyczy M, Kaszaki J, Boros M, Hideghéty K. (2014) Peripheral inflammatory activation after hippocampus irradiation in the rat. Int J Radiat Biol 90: 1–6.
IF: 1.895

II. Torok R, Torok N, Szalardy L, **Plangar I**, Szolnoki Z, Somogyvari F, Vecsei L, Klivenyi P. (2013) Association of vitamin D receptor gene polymorphisms and Parkinson's disease in Hungarians. Neurosci Lett 551: 70–74.
IF: 2.026

III. Szalardy L, Zadori D, **Plangar I**, Vecsei L, Weydt P, Ludolph AC, Klivenyi P, Kovacs GG. (2013) Neuropathology of partial PGC-1α deficiency recapitulates features of mitochondrial encephalopathies but not of neurodegenerative diseases. Neurodegener Dis 12: 177–188.

IF: 3.056

IV. **Plangar I**, Majlath Z, Vecsei L. (2012) Kynurenines in cognitive functions: their possible role in depression. Neuropsychopharmacol Hung 14: 239–244.

V. Vecsei L, **Plangar I**, Szalardy L. (2012) Manipulation with kynurenines: a possible tool for treating neurodegenerative diseases? Expert Rev Clin Pharmacol 5: 351–353.

VI. **Plangár I,** Zádori D, Klivényi P, Toldi J, Vécsei L. (2011) Targeting the kynurenine pathway-related alterations in Alzheimer's disease: a future therapeutic strategy. J Alzheimers Dis 24: 199–209.

IF: 3.745

VII. Zádori D, Klivényi P, **Plangár I,** Toldi J, Vécsei L. (2011) Endogenous neuroprotection in chronic neurodegenerative disorders: with particular regard to the kynurenines. J Cell Mol Med 15: 701–717.

IF: 4.125

VIII. **Plangár I**, Zádori D, Klivényi P, Toldi J, Vécsei L. (2009) The role of the kynurenine pathway in neurodegeneration and neuroprotection. Publication of the Proceedings of the 7th International Congress on the Improvement of the Quality of Life on Dementia, Parkinson's Disease, Epilepsy, MS and Muscular Disorders and Neuroethics. Bologna: Medimond Monduzzi Editore, pp. 21–26, Thessaloniki, Greece.

IX. Varga H, Pardutz A, Vamos E, **Plangar I**, Egyud E, Tajti J, Bari F, Vecsei L. (2007) Cox-2 inhibitor attenuates NO-induced nNOS in rat caudal trigeminal nucleus. Headache 47: 1319–1325.

IF: 2.358

Total impact factor: **17.205**

Cumulative impact factor: 22.717

TABLE OF CONTENTS

LIST OF ABBREVIATIONS

3D – 3 dimension

ABC – ATP-binding cassette

AD – Alzheimer's disease

AMPA – α-amino-3-hydroxy-5-methyl-4-isoxazolepropionic acid

ANOVA – analysis of variance

AP – allopurinol

ATP – adenosine triphosphate

AX – axial

BBB – blood-brain barrier

BCSFB – blood-cerebrospinal fluid barrier

bw – body weight

CNS – central nervous system

CO – control

CT – computed tomography

IR-FSPGR – inversion recovery prepared fast spoiled gradient recalled sequence

DA – dopamine

DOPAC – 3,4-dihydroxyphenylacetic acid

EAA – excitatory amino acid

EDTA - disodium ethylenediaminetetraacetate

FOV – field of view

GPC – L-alpha-glycerylphosphorylcholine

GSH – glutathione

GSSG – glutathione disulphide

H&E – haematoxylin–eosin

HPF – high-power field

HPLC – high-performance liquid chromatograpy

HVA – homovanillic acid

i.p. – intraperitoneal

KYNA – kynurenic acid

LDRI – radiation-induced delayed brain injury

L-KYN – L-kynurenine

MPP^+ – 1-methyl-4-phenylpyridinium

MPTP – 1-methyl-4-phenyl-1,2,3,6-tetrahydropyridine

MRI – magnetic resonance imaging

MRP – multidrug resistance-associated protein

MS – multiple sclerosis

MU – monitor unit

MWM – Morris water maze

NGN – naringenin

NMDA – N-methyl-D-aspartate

OM – optical magnification

PBS – phosphate-buffered saline

PD – Parkinson’s disease

PFA – paraformaldehyde

P-gp – P-glycoprotein

QOL – quality of life

QUIN – quinolinic acid

RT – radiation-treated

SAG – sagittal

SEM – standard error of the mean

SIL – silymarin

SNpc – substantia nigra pars compacta

Sp – space

SP – sulfinpyrazone

SPRD – Sprague-Dawley

SRS – stereotactic radiosurgery

SSD – source-to-skin distance

ST – slice thickness

T1 – longitudinal relaxation time

T2 – transverse relaxation time

T1W – T1-weighted

T2W – T2-weighted

TE – echo time

TI – inversion time

Tr – repetition time

SUMMARY

In the present work, the processes of neurodegeneration and radiation-induced brain injury and potential neuroprotection are examined in small-animal models. There are a number of characteristics in common between neurodegenerative disorders and radiation-related brain injury. Both are characterized by progressive neuronal cell death, and motor and cognitive functional damage. Neurodegenerative disorders and irradiation are similar in the various associated degrees of inflammation. The time course from the initiation of neuronal cell death to the appearance of clinical symptoms varies, but a period of decades generally passes before an overwhelming number of neurones are affected, which opens up therapeutic possibilities, the aim being to halt further neuronal loss. Inflammatory cells often appear in the vicinity of the affected neurones, their presence ranging from robust in Alzheimer's disease (AD) to relatively slight in Parkinson's disease (PD).

PD is one of the most common neurodegenerative disorders. Despite recent and continuous advances in research, the precise pathomechanism and the unambiguous causes of this disease remain unclear. Administration of environmental toxins, e.g. 1-methyl-4-phenyl-1,2,3,6-tetrahydropyridine (MPTP), can trigger a similar, but not identical clinical picture, not only in humans, but also in rodents. In mice, MPTP, or rather its active metabolite, 1-methyl-4-phenylpyridinium (MPP^+), primarily kills the dopamine (DA)-producing neurones in the substantia nigra pars compacta (SNpc), inhibits mitochondrial respiration at complex I and induces oxidative stress, which lead to further cell destruction.

Radiation-induced brain injury often appears after partial or whole brain irradiation and involves both anatomic and functional deficits. Until the 1970s, the human brain was thought to be highly radioresistant, but later preclinical studies have provided evidence of radiation-induced severe impairments in memory, attention and other cognitive dysfunctions which have profound effects on the quality of life (QOL). We therefore set out to establish an effective small-animal focal brain radiation model for research on brain injuries and to develop new potential therapeutic strategies. With this aim, we first developed a precise dose delivery technique for partial brain irradiation of 2 rats simultaneously, using a stereotactic frame of the BrainLab system. We later described a method which permits precise dose delivery to a definite part of one hemisphere of the brain for 6 rats at a time.

In a search for potential therapeutic approaches, we first tested several inhibitors and stimulators of transport proteins localized at the blood-brain barrier (BBB). It was anticipated that

stimulation of the multidrug resistance-associated protein 1 (MRP1)- and MRP2-mediated transport of glutathione (GSH) conjugates of toxic substances may have slight beneficial effects, whereas stimulation of the MRP4-mediated efflux of brain urate, which has important antioxidant potency, may worsen the effects of oxidative stress. These data may contribute to a better understanding of the pathomechanisms of PD and the relevance of the excitotoxic and neuroinflammatory processes in these conditions.

Thereafter, in the knowledge that the overactivation of excitatory amino acid (EAA) receptors plays an important part in the pathomechanism of various neurodegenerative diseases, we would have wished to investigate the EAA receptor antagonist kynurenic acid (KYNA) and its novel synthetized derivatives. KYNA is an endogenous product of the tryptophan metabolism and may serve as a protective agent in neurological disorders. However, we had to exclude the use of KYNA, because it is almost unable to pass through the BBB, whereas the newly synthetized analogues can readily cross this barrier and exert their complex anti-excitatory activity. Behavioural studies with these KYNA amides proved that they do not provoke significant non-specific general side-effects.

In our advanced partial brain radiation model, the development of morphological and functional changes proved to be dose-dependent. To test the spatial learning and memory and to detect early functional impairment of the rat brain, the Morris water maze (MWM) task proved to be perfect tool. With the aid of magnetic resonance imaging (MRI) screening, we could define the time point for histological examinations. The applied model permits accurate dose delivery to a specified region in one hemisphere of the brain for 6 rats at a time. Following complex research, a dose of 40 Gy and a follow-up time of 4 months are suggested for investigations on neuroradiation modifiers. Primarily the water-soluble, deacylated phosphatidylcholine derivative L-alpha-glycerylphosphorylcholine (GPC) improved both the cognitive functions and the learning and memory capacity.

Although the precise pathomechanism of PD and the processes involved in the development and progression of radiation-induced cognitive impairment remained unclear, it is clear that there are several agents which can modify the course of the disease or mitigate the late effects in preclinical models.

I. INTRODUCTION

There may be a considerable number of harmful effects in the background of neuronal damage, caused by several different diseases of the nervous system. These damaging factors may be traumas, vascular disturbances, physical impacts (e.g. irradiation), toxic effects, inflammation and autoimmune, degenerative or tumourous processes.

Neurodegenerative diseases are severe disorders which primarily affect the nervous system. Since the aetiology and precise pathomechanism of these diseases are unknown, the treatment poses a great challenge for basic science and clinical investigations.

Radiation therapy is an important part of the complex management of primary and secondary brain tumours. Sadly, the incidence of brain tumours has become more significant over the years, and therapeutic strategies to prevent or mitigate radiation-induced cognitive impairment have therefore increased in importance.

There are a number of similarities between neurodegenerative disorders and radiation-induced brain injury. BBB disruption is one of the major consequences of radiation-induced normal tissue injury (Lee et al. 2012) in the central nervous system (CNS) and disruption of the neurovascular system has been proved in most neurodegenerative disorders too (Lin et al. 2013; Lee & Pienaar 2014). The main mutual feature is that both finally lead to neuronal cell death. The loss of neurones is progressive and irreversible, but the temporal appearance of the consequences may differ considerably. The time which passes from the initiation of neuronal cell death to the appearance of clinical symptoms can vary somewhat, but a period of decades generally passes before an overwhelming number of neurones are affected (Bredesen et al. 2006). Inflammation with varying degrees of severity can be observed in both cases (Flood et al. 2011; Khandelwal et al. 2011; Moore et al. 2013). The other important similarity is the impairment of both motor and cognitive functions. The functional and morphological changes often coexist. However, their distinction can be difficult, and the detection of molecular, cellular and microanatomic changes help to unravel the puzzle and facilitate an understanding of the processes in the background of the disorders.

In the present work, we chose to examine PD, a progressive disorder with functional abnormalities that lead to dementia. The behavioural changes, loss of memory, and histological and cellular disturbances caused by irradiation strongly resemble the changes caused by neurodegenerative processes. In both cases, it is essential to make use of small-animal models in order to perform complex investigations, including neurofunctional and morphological examinations, with potentially neuroprotective, radio-neuroprotective agents. For these reasons, in the present

work we investigated these two at first sight not closely related topics, neurodegeneration and radiation-induced brain injuries, in light of the fact that neuroinflammation and impairment of the BBB may occur in both.

I.1. Parkinson's disease

PD, the second most common progressive neurodegenerative disorder after AD (Tanner & Goldman 1996), affects approximately 1% of the population older than 65 years (Gibrat et al. 2009). It is characterized by a predominance of severe motor dysfunctions and autonomic, psychiatric and cognitive disturbances resulting from the loss of DAergic neurones in the SNpc (Hirsch et al. 1988) and depletion of DA in the striatum (Savitt et al. 2006; Agid 1991). Despite intensive research, the distinct cellular and molecular pathomechanism of PD remains largely unclear. It is well known that impairment of the mitochondrial respiratory chain at the level of complex I plays a pivotal role in the pathomechanism (Reichmann & Riederer 1989; Schapira et al. 1989). MPTP is highly lipophilic and rapidly crosses the BBB, a physical and metabolic barrier which prevents circulating drugs and toxins from entering the brain (Markey et al. 1984). MPTP is a neurotoxin precursor to the complex I inhibitor MPP^+, which selectively destroys the DAergic neurones in the SNpc in human and non-human primates, with a resulting decline in striatal DA content (Dauer & Przedborski 2003). Indeed, administration of MPTP causes permanent symptoms of PD, irreversible neurodegeneration, and in mice also results in the appearance of the characteristic biochemical and histological features of the human cases (Hallman et al. 1984; Langston et al. 1999). As a consequence, a mouse model of MPTP intoxication is the most extensively used animal model of human PD.

I.2. Radiation-induced brain damage

The incidence of CNS tumours is constantly rising. Radiotherapy is an indispensable part of standard complex therapy in the cases of both primary and secondary brain tumours. Radiation-induced brain injury is a severe, untreatable and irreversible complication of radiation-treated (RT) malignant brain tumours and prevents the effective treatment of malignant CNS tumours.

There is cumulative evidence in the literature that the same factors may play roles in the pathomechanism of both multiple sclerosis (MS) and radiation-related injuries of the brain. In both cases, axonal damage and necrosis are the main features responsible for the neurological disabilities and serious consequences of irradiation. The causes and pathogenesis of axonal damage in MS and late radiation injury are still obscure, but there is a growing body of information indicating that both

inflammation and demyelination may play a major role in the process (Kreitman and Blanchette 2004; Na et al. 2013).

Radiogen necrosis is frequently associated with appreciable functional morbidity and a declining QOL in patients treated with brain radiotherapy. In cases of primary CNS tumours and in the palliation of metastatic tumours, the brain is one of the most generally irradiated sites for curing. Since higher radiation doses to the tumour can elevate local tumour control and improve the entire prognosis, radiation dose schemes have changed over the last few decades. Radiation dose escalations have been the most extensively applied dose schemes in recent years. With these disturbances, severe damage to the parenchyma of the normal brain has become one of the inevitable consequences (Tsien et al. 2009; Floyd et al. 2004; Roberge et al. 2009; Beşe et al. 1998). The dose which would most probably destroy the tumour can not be delivered by reason of the low radiation tolerance of the brain and spinal cord. The emerging new techniques, such as stereotactic radiosurgery (Simon et al. 2007), intensity-modulated brachytherapy (Shi et al. 2010), conformal and intensity-modulated teletherapy and proton therapy, increase the physical selectivity of the dose delivery (Attanasi et al. 2008). However, surrounding normal brain tissue must be included in the clinical target volume, because of the potential tumour cell content. An active neuroprotective agent could therefore theoretically increase the therapeutic index, providing the prospective of an improved outcome of irradiation or combined chemoradiation. It may lead to ameliorated local control and consequently prolonged survival for patients with a high-grade astrocytoma or glioblastoma multiforme. The incidence of radiation damage depends on the total dose and the rate of delivery (fractionation) (Prasad 2005). Oedema, vasculopathy, infection and chemotherapy potentiate radiation injury. Post-irradiation reactions in the CNS are well described as acute, subacute and late CNS reactions. Tumours predispose to these normal tissue reactions by the oedema and pressure epiphenomena that occur in their environs, and probably by other mechanisms associated with tissue breakdown. Radiation-induced delayed brain injury (LDRI) is a well-documented complication that occurs 4 months to 10 years after radiation therapy (70% of cases occur in the first 2 years) (Greene-Schloesser et al. 2013). The incidence of LDRI is 5–37% and increases with higher radiation doses. In the lack of effective treatment, LDRI can cause progressive deterioration and death; however, the cause of this damage has not been determined. The primary mechanism of LDRI involves a vascular endothelial injury or direct damage to the oligodendroglia. Cytokines and growth factors are important regulatory proteins controlling the growth and differentiation of normal and malignant glial cells, which have been implicated in the tissue response to radiation injury. The white matter is affected more than the grey matter (Shi et al. 2009). The histopathologic examination of post-irradiation specimens demonstrates variable

amounts of gliosis, tissue necrosis, calcification, inflammation, and vascular proliferation and hyalinization, and also diffuse T-cell infiltration with both CD4+ and CD8+ cells. Infiltrating activated macrophages (CD11c+, HLA-DR+) and tumour necrosis factor-alpha and interleukin-6 immunoreactivity are predominately localized to the macrophages (Kureshi et al. 1994).

If an effective neuroprotective drug were available, the therapeutic index (the ratio of the anti-tumoural effect and the side-effects) could be changed substantially. The histological and cellular disturbances caused by irradiation closely resemble the neurodestructive changes and neuronal death manifested as a result of neurodegenerative processes. Numerous other studies have suggested that neurocognitive deficits and an intellectual decline which severely affect the patient's QOL similarly occur following whole or partial brain irradiation (Roman and Sperduto 1995; Greene-Schloesser et al. 2013). Following the incorporation of adjunctive chemoradiation into the standard treatment regimen for patients with glioblastoma, many trials have confirmed both histopathologically and radiographically up to a 3-fold elevation in the number of treatment-related injuries as compared with radiation alone (de Wit et al. 2004; Chamberlain et al. 2007; Brandsma et al. 2008).

I.3. Therapeutic approaches

I.3.1. ABC transporters and subfamily of MRPs

Recent investigations have attracted attention to the roles of the dysfunction of the BBB and the blood-cerebrospinal fluid barrier (BCSFB) in neurodegenerative disorders. Passage across these barriers is modulated by certain transport proteins and pumps. Many of the efflux pumps belong in the adenosine triphosphate (ATP)-binding cassette (ABC) transporter superfamily, one of the largest and most ancient families of transmembrane proteins. These proteins bind ATP and utilize the energy of ATP hydrolysis to perform transporter functions. The classification is based on the sequence and organization of their nucleotide binding fold or ATP-binding domain (van Veen & Konings 1998). In humans, certain ABC transporters are principal causes of resistance of cancers to chemotherapy and are involved in cystic fibrosis and a range of other inherited human diseases.

The functioning of these transporters moderately influences the bioavailability and disposition of many substances (Ayrton & Morgan 2001) by limiting the uptake of drugs or toxins into the target cells and also restricting the tissue accumulation of toxic endogenous metabolites (Silverman 1999). The ABC transporters can be subdivided into 7 groups, ABCA–G (Borst & Elferink 2002). As regards the pathogenesis and treatment of neurological disorders, perhaps the most widely studied ABC transporter is P-glycoprotein (P-gp) or human ABCB1 (Lee & Bendayan

2004). This is localized on both the luminal (endothelial cells) (Beaulieu et al. 1997) and abluminal (astrocyte foot processes) (Golden & Pardridge 1999) sides of the BBB, and the subapical side of the choroid plexus epithelia in the BCSFB (Rao et al. 1999). The accumulation of toxic substances in the brain may be due to the disruption of P-gp expression at the BBB (Schinkel et al. 1994), thereby heightening the risk of neurological disorders, e.g. PD (Drozdzik et al. 2003). However, it has been demonstrated that MPP^+ is not a P-gp substrate (Staal et al. 2001).

Increasing attention has recently been paid to the role of MRPs or human ABCCs in neurological disorders (Dallas et al. 2006). The data obtained from studies using murine models of neurodegenerative diseases, such as AD (Krohn et al. 2011), suggest that MRPs may play an important role in the neurodegenerative process too. However, there are only a few arguments in favour of the involvement of MRPs in PD pathogenesis (Le Couteur et al. 2001). Abundant data are available as regards the localization and function of MRPs in the brain, with some controversies. MRP1 has been demonstrated to be expressed on the luminal/abluminal side of the human and rodent BBB (Nies et al. 2004; Soontornmalai et al. 2006; Roberts et al. 2008) and on the basolateral side of the human and rodent choroid plexus (Soontornmalai et al. 2006; Roberts et al. 2008; Nishino et al. 1999). Although MRP1-mediated efflux in the murine BBB is questionable (Cisternino et al. 2003), it seems to be fully functional in the BCSFB (Wijnholds et al. 2000). MRP1 is capable of transporting GSH and oxidized GSH (GSSG) and GSH conjugates of certain substances (Zhou et al. 2008). For example, the GSH conjugate of 4-hydroxy-*trans*-2-nonenal, a chemically reactive and prevalent toxic aldehyde, is also transported by MRP1 (Renes et al. 2000), which would be an important detoxification mechanism during oxidative stress. However, free GSH can also be depleted by MRP1, a process of unclear significance which can be stimulated by bioflavonoids, e.g. naringenin (NGN) (Leslie et al. 2003). The function of MRP1 can be inhibited by several substances, including silymarin (SIL) (Wu et al. 2005), probenecid (Gollapudi et al. 1997) and sulfinpyrazone (SP) (Bakos et al. 2000). Although MRP2 is widely expressed in the luminal surface of the capillary endothelium in the porcine and rodent brain (Miller et al. 2000), its functional presence in the human brain is equivocal. It has been demonstrated by the use of cDNA arrays to be overexpressed in endothelial cells from temporal lobe blood vessels of patients with refractory epilepsy (Dombrowski et al. 2001), and polymerase chain reaction analysis showed the expression of MRP2 mRNA in perilesional tissue from patients with brain glioma or cerebral haemorrhage (Nies et al. 2004), but the MRP2 protein itself could not be detected by immunofluorescence microscopy in those perilesional tissues (Nies et al. 2004). The substrates of MRP1 and MRP2 show similarity with regard to the transport of GSH, but the affinity of MRP2 for GSH conjugates is less than that of MRP1 (Evers et al. 2000). MRP2-mediated transport can also be

stimulated by NGN, and interestingly, in contrast with MRP1, SP also stimulates it (Pedersen et al. 2008). The function of MRP2 can be inhibited by numerous substances, including SIL (Pedersen et al. 2008). Although quantitative polymerase chain reaction analysis indicated the brain expression of MRP3 mRNA, which shows the highest amino acid sequence resemblance (58%) with MRP1 (Kiuchi et al. 1998), the protein itself is not synthesized in detectable amounts in the brain (Nies et al. 2004). MRP4 and MRP5 isoforms seem to be the major MRP isoforms synthesized in the human brain (Nies et al. 2004). MRP4 has been demonstrated to be localized in the luminal surface of the human and rodent BBB (Nies et al. 2004; Roberts et al. 2008; Leggas et al. 2004) and on the basolateral side of the human and rodent choroid plexus (Roberts et al. 2008; Leggas et al. 2004; Choudhuri et al. 2003). Although MRP5 has been reported to be clearly localized to the luminal side of the BBB in human brain, it exhibits only a low expression level in the rodent BBB (Roberts et al. 2008). As regards the BCSFB, MRP5 is mainly localized to the ependymal cells in the rodent brain (Roberts et al. 2008). MRP4 and MRP5 have similar substrate specificities and can transport molecules involved in cellular signalling, such as cyclic nucleotides (Zhou et al. 2008), while MRP4 can also transport purine metabolites, such as urate (Van Aubel et al. 2005). Allopurinol (AP), a well-known purine analogue and xanthine oxidase inhibitor, has been demonstrated to be an allosteric enhancer of MRP4-mediated transport (El-Sheikh et al. 2008), while NGN is capable of moderate stimulation of the ATPase activity of the transporter (Wu et al. 2005). SP and SIL are able to inhibit both MRP4- and MRP5-mediated transport, to similar extents, while probenecid is a considerably more potent inhibitor of MRP5 than of MRP4 (Wu et al. 2005; Reid et al. 2003).

Probenecid is a widely-used non-selective inhibitor of MRPs and organic anion transporters (Zhou et al. 2008; Sugiyama et al. 2001). Probenecid treatment enhances the toxicity of MPTP, which is presumably due to the inhibitory effect of probenecid on MPTP transport in the kidney and BBB (Lau et al. 1990; Meredith et al. 2008).

The few available data as regards the role of MRPs in PD led us to investigate the possible roles of MRPs in the neurotoxicity of MPTP/MPP^+. As there are no specific and selective inhibitors or stimulators of MRPs that are available for *in vivo* and *in vitro* studies, we applied SIL as an inhibitor of MRP1, MRP2, MRP4 and MRP5, NGN as a stimulator of MRP1, MRP2 and MRP4, SP as an inhibitor of MRP1, MRP4 and MRP5 and a stimulator of MRP2, and AP as an MRP4 stimulator.

I.3.2. Kynurenic acid analogues

It is well known that excitotoxicity, which means an extreme high glutamate level in the brain, is in the background of numerous neurodegenerative processes. During pathological events, neurones are impaired or killed by the overactivation of EAA receptors such as N-methyl-D-

aspartate (NMDA), α-amino-3-hydroxy-5-methyl-4-isoxazolepropionic acid (AMPA) and kainate (Olney 1969). The metabolites which can result from the oxidative metabolism of tryptophan and mainly the kynurenine pathway can change the excitability of brain tissue. Those compounds which inhibit quinolinic acid (QUIN), the glutamate receptor agonist intermediate of the tryptophan metabolism, and also free radical-generated effects, might be potentially neuroprotective. KYNA exerts an antagonistic effect on the NMDA receptors at the glycine binding site (Kessler et al. 1989) thereby decreasing the free radical formation-induced neurotoxic effects of QUIN and its precursor 3-hydroxy-L-kynurenine, which primarily develop in the neocortex, striatum and hippocampus. These regions are the predilection sites of neurodegenerative diseases. L-Kynurenine (L-KYN), the precursor of KYNA, and some KYNA derivatives can pass through the BBB. These compounds can efficiently inhibit brain injuries following hyperexcitability, and hence in appropriate concentration can be neuroprotective, as proved by the attenuation of different noxae (e.g. in cerebral ischaemia, pentylenetetrazole-induced epileptic seizure and experimental migraine or Huntington models). Those experimental results are likewise very important which suggest that L-KYN and its metabolites influence the cerebral blood flow and its vasodilative effect can facilitate neuroprotective processes (Bari et al. 2006). Following radiation-stimulated inflammatory reactions of the CNS, which restrict the effective therapy of brain tumours, and the selective decline of progressive neuronal death caused by microglia degeneration and the impaired circulation of the blood supply, KYNA analogues might theoretically be well applicable.

In recent years, several KYNA derivatives have been developed, among them KYNA amides. One of the new analogues, N-(2-N,N-dimethylaminoethyl)-4-oxo-1H-quinoline-2-carboxamide hydrochloride (KYNA-1), has proved to be neuroprotective in several models. One of our papers reports on the synthesis of 10 new KYNA amides (KYNA-1–KYNA-10) and on the effectiveness of these molecules as inhibitors of excitatory synaptic transmission in the CA1 region of the hippocampus. The molecular structure and functional effects of KYNA-1 are compared with those of other KYNA amides. KYNA-1 may be considered a promising candidate for clinical studies.

I.3.3. Potentials in a phosphatidylcholine derivative

Phosphatidylcholine is a key component of endogenous surface-coating substances and biomembranes, and it is well founded that this is the main constituent involved in lipid peroxidation and the loss of membrane-forming phospholipid bilayers (Volinsky & Kinunnen 2013). GPC is a water-soluble, deacylated phosphatidylcholine derivative which may be hydrolysed to choline and can possibly be applied for the resynthesis of phosphatidylcholine (Gallazzini & Burg 2009). Interestingly, markedly lower levels of GPC have been reported after experimental haemorrhagic

shock, with recovery to the baseline only 24 h later (Scribner et al. 2010). Several lines of research suggest that GPC would be efficacious in influencing the inflammatory response. GPC has proved effective against loss of the membrane function in CNS injuries (Amenta et al. 1994; Onishchenko et al. 2008), and it was previously investigated as a centrally acting parasympathomimetic drug in acute cerebrovascular diseases and dementia disorders (Barbagallo Sangiorgi et al. 1994; De Jesus Moreno Moreno 2003; Parnetti et al. 2007). After oral administration, GPC has been demonstrated to pass through the BBB and reach the CNS, where it is incorporated into the phospholipid fraction of the neuronal plasma membrane and microsomes (Tayebati et al. 2011). Brownawell et al. (2011) studied the toxicity of GPC in rodents. The acute, subacute and late effects of different GPC doses in the range from 100 mg/kg body weight (bw) to 1000 mg/kg bw have been examined in rats. Acutely, the lethal dose of intravenously injected GPC was 2000 mg/kg, and the intraperitoneal (i.p.) dosing of rats resulted in mortality starting at 1500 mg/kg. In subchronic or chronic studies, doses of 100 and 300 mg/kg GPC did not modulate the body weight, behaviour, clinical chemistry or haematology of rats, and did not produce any signs of general toxicity.

II. AIMS

Our aim was to develop reproducible preclinical models in order to test different approaches and compounds which may protect against damage caused by neurotoxic agents.

We set out to determine tolerability and possible toxic effects of promising neuroprotectors.

Additionally, we proposed an integrated system of behavioural, histological and molecular investigations on correlations of the early and late changes caused by ionizing radiation.

After establishment of this small-animal model, our goal was to explore the pathomechanism of radiation changes and research on potential neuro-radioprotective agents.

In summary, the aims of our studies were:

(i) an assessment of the roles of certain MRPs (1, 2, 4 and 5) in the neurotoxicity induced by MPTP;

(ii) to examine whether KYNA amides exert any behavioural side-effects in the C57B/6 mouse strain;

(iii) to develop a precise dose delivery technique for partial brain irradiation and to set up a small-animal model of ionizing radiation-induced brain injury;

(iv) to set up a dose–effect curve of radiosensitivity and to establish the most appropriate dose of irradiation for research on radiation modifiers;

(v) to investigate late effects of radiation-induced brain injuries; and

(vi) to apply the model to investigate potential radiation-induced brain injury modifiers.

III. MATERIALS AND METHODS

III.1. Drugs

NGN, SIL, SP, AP, sesame oil, MPTP, DA hydrochloride, 3,4-dihydroxyphenylacetic acid (DOPAC), homovanillic acid (HVA), sodium metabisulphite and sodium octylsulphate were from Sigma-Aldrich Hungary Ltd. (Budapest, Hungary). Perchloric acid, disodium ethylenediaminetetraacetate (EDTA), sodium dihydrogenphosphate, acetonitrile and phosphoric acid were from VWR International Ltd. (Debrecen, Hungary).

L-KYN sulphate (KYNA-11) was from Sigma-Aldrich Hungary Ltd. (Budapest, Hungary). New KYNA amide derivatives (KYNA-1, N-(3-N,N-dimethylaminopropyl)-4-oxo-1H-quinoline-2-carboxamide hydrochloride (KYNA-2) and N-(2-N-pyrrolidinylethyl)-4-oxo-1H-quinoline-2-carboxamide hydrochloride (KYNA-6)) were prepared from KYNA and the appropriate amine by using N,N-diisopropylcarbodiimide as coupling reagent.

GPC was produced by Lipoid GmbH (Ludwigshafen, Germany).

III.2. Behavioural studies

III.2.1. Open-field

The spontaneous locomotor and exploration activities were measured by an automated tracking system with an activity chamber. The open black box with a dark floor was made of wood. The box was connected to a computer which recorded the inquisitive behaviour and locomotor activity of the animal. Each animal were placed individually at the centre of the black box (48 x 48 x 40 cm), which was equipped with automated infrared photocells for measurements, and allowed to move spontaneously for 5 (in the case of mice) or 15 (in the case of rats) minutes. The tests were performed at the same time of day so as to minimize changes due to the diurnal rhythm. Between sessions, the arena was cleaned with 70% alcohol and dried. The movement signals were analysed by Conducta 1.0 (Experimetria Ltd, Budapest, Hungary) software. The analysis resulted in a track record; the locomotor activity was expressed as the total distance moved (cm) in a predetermined period of time, the times spent in movement and at rest (s), the mean velocity (cm/s), and the frequency and duration of rearing.

In the course of the studies of the behavioural effects of KYNA analogues, the mice were examined 2 h after the first treatment (acute), and then on the last day (day 9) of treatment (chronic). In this case, the ambulation time, the mean velocity, the local time and the number of rearings were evaluated. In the other experiments, rats were tested every 2 weeks and the ambulation distance, velocity, immobility time and rearing count were assessed.

III.2.2. Morris water maze test

The MWM protocol of Vorhees and Willams (Vorhees and Williams 2006) was used, visuospatial cues being provided to guide the animals in tests of hippocampal memory. The MWM consisted of a cylindrical white tank with a diameter of 175 cm and a height of 50 cm, containing liquid made opaque with a non-toxic white dye. The tank was filled with water up to 32.5 cm and maintained at 21–24 °C. The pool was divided into four equal quadrants, and a removable transparent Plexiglas platform (10 cm in diameter) that could not be seen by the swimming rats was hidden at the centre of one of the quadrants, with its top 1 cm below the surface. The platform provided the only escape from the water. The position of the platform was constant throughout the 3-day acquisition period. Pictures fixed permanently on the surrounding walls served as distal navigation cues to enable the rats to locate the platform. The distinctive visual cues remained constant throughout the entire course of testing. The first two days were acquisition or training days, and the task was performed on the third day. The training period consisted of 4 trials per day with a 5-min inter-trial interval. Each trial began with the rat in the pool and ended when the rat found the platform or after 120 s. If the animal failed to locate the platform within 120 s, it was guided to the platform manually. Once on the platform, the rat was allowed to rest for 10 s. It was then towel-dried and placed in an inter-trial holding cage where a heating source was provided to maintain the animal's body temperature during the inter-trial interval. During the acquisition phase, measurements were made of the time (s) and the path length (cm) taken to locate the platform. This site navigation test was performed once before the irradiation and subsequently once in the third and once in the fourth month.

III.3. Animal model of PD

III.3.1. Animals

The procedures utilized in this study followed the guidelines of the European Communities Council (86/609/ECC) to minimize animal suffering and were approved in advance by the Ethics Committee of the Faculty of Medicine, University of Szeged. Six-week-old C57B/6 male mice (weighing between 18 and 23 g) were used. The animals were housed in cages (at most 5 per cage) and maintained under standard laboratory conditions, with tap water and regular mouse chow available *ad libitium* on a 12 h light-dark cycle, at 21±1 ºC and 50±10% humidity.

III.3.2. Treatments

Four groups of mice were used in the first 4 experimental set-ups for the assessment of the 4 substances. The first 2 groups of mice received i.p. injections of SIL (100 mg/kg/day, in a volume of 5 ml/kg, suspended in sesame oil; n_1=8, n_2=9), NGN (100 mg/kg/day, in a volume of 5 ml/kg,

suspended in sesame oil; n_1=7, n_2=7), SP (100 mg/kg/day, in a volume of 5 ml/kg, suspended in sesame oil; n_1=8, n_2=9) or AP (60 mg/kg/day, in a volume of 5 ml/kg, suspended in sesame oil; n_1=10, n_2=10) respectively, once a day, at the same time each day for one week. The second 2 groups of mice received sesame oil (in a volume of 5 ml/kg; n_3=8, n_4=8; n_3=7, n_4=7; n_3=8, n_4=9; n_3=6, n_4=10) in the same treatment regime. On day 8 of the experiments, 1 h after the regular daily injections, the second and fourth groups received i.p. injections of MPTP (15 mg/kg, in a volume of 5 ml/kg, dissolved in 0.1 M phosphate-buffered saline (PBS)) 5 times at 2 h intervals (total dosage: 75 mg/kg). The first and third groups received 0.1 M PBS (in a volume of 5 ml/kg) in the same treatment regime. From day 9, the 4 substances were further administered once a day for another week, with the corresponding control injections, according to the treatment regime detailed above.

III.3.3. Sample preparation

Eight days after toxin administration (day 16 of the experiment), all the mice were decapitated and the brains were rapidly removed and placed on an ice-cooled plate for dissection of the striatum. After dissection of both striata from the forebrain block, these were stored at −70 °C until further sample processing. In the next step, the striata were weighed and then manually homogenized in an ice-cooled solution (250 µl) comprising perchloric acid (7.2 µl; 70% w/w), sodium metabisulphite (1 µl; 0.1 M), EDTA (1.25 µl; 0.1 M) and distilled water (240.55 µl) for 1 min in a homogenization tube. The content of the homogenization tube was washed quantitatively into a polypropylene Eppendorf tube with the used solution to give a final volume of 1.5 ml, which was then centrifuged at 10,000 g for 15 min at 4 °C. Thereafter, the supernatant was transferred to another polypropylene Eppendorf tube and was stored at −70 °C until chromatographic analysis.

III.3.4. Chromatographic conditions

DA and its metabolites, DOPAC and HVA, were analysed by reversed-phase chromatography, using an Agilent 1100 high-performance liquid chromatography (HPLC) system (Agilent Technologies, Santa Clara, CA, USA) combined with a Model 105 electrochemical detector (Precision Instruments, Marseille, France) under isocratic conditions. In brief, the working potential of the detector was set at +750 mV, using a glassy carbon electrode and an Ag/AgCl reference electrode. The mobile phase containing sodium dihydrogenphosphate (75 mM), sodium octylsulphate (2.8 mM) and EDTA (100 µM) was made up with acetonitrile (7% v/v) and the pH was adjusted to 3.0 with phosphoric acid (85% w/w). The mobile phase was delivered at a rate of 1 ml/min at 40 °C onto the reversed-phase column (HR-80 C18, 80×4.6 mm, 3 µm particle size; ESA Biosciences, Chelmsford, MA, USA) after passage through a pre-column (Hypersil ODS, 20x2.1 mm, 5 µm

particle size; Agilent Technologies, Santa Clara, CA, USA). Ten-microlitre aliquots were injected by the autosampler with the cooling module set at 4 °C. The signals captured by the Model 105 electrochemical detector were converted by an Agilent 35900E dual-channel interface and the chromatograms were evaluated by ChemStation Rev.1.10.02 software (Agilent Technologies, Santa Clara, CA, USA).

III.4. Study of behavioural effects of some kynurenic acid analogues

III.4.1. Animals

Behavioural experiments were carried out on 6-week-old C57B/6 male mice (n=60). The animals were kept under controlled environmental conditions at 22±2 ˚C under a 12-h light-dark cycle. Food and water were available *ad libitum*. The local Animal Ethics Committee had approved all experiments. The care and use of the experimental animals were in full accordance with the 86/609/EEC directive.

III.4.2. Treatment regime

The mice received i.p. injections of KYNA-1 (200 mg/kg/day, in a volume of 5 ml/kg, dissolved in distilled water, the pH of which was adjusted to 6.5 with 1 N NaOH). For comparison, KYNA-2 or KYNA-6 in equimolar dosages (likewise in a volume of
5 ml/kg, dissolved in distilled water, the pH of which was adjusted to 6.5 with 1 N NaOH) or the vehicle (0.1 M PBS, in a volume of 5 ml/kg) was administered at the same time each day from 6 weeks of age.

In behavioural experiments, the mice were treated once (in acute experiments) or for 9 days (in chronic experiments) according to the regime detailed above.

III.5. Small-animal model of irradiation

III.5.1. Animals

Experiments were performed on 57 adult Sprague-Dawley (SPRD) male rats, weighing on average 210 g (range 176–280 g). The animals were housed in a climate-controlled environment (25 °C) maintained on a 12 h light/12 h dark cycle and were allowed free access to food and water. All experiments were conducted in full accordance with the European Communities Council Directive (86/609/EEC) for the Care and Use of Laboratory Animals and were approved by the University Animal Research Committee.

III.5.2. Dosimetry of small electron field

In order to verify the dose depth curve, the field profile and the lateral dose fall-off of the 2, 4, 6, 8, 10 and 12 mm electron collimators, we measured the absorbed dose of a 6 MeV electron beam irradiating at a dose rate of 300 monitor units (MU)/min in a water phantom, using a pin-point ionization chamber (Canberra Packard Central Europe GmBH, Schwadorf, Austria), and in a solid water phantom with a 1 cm build-up layer for film dosimetry (Canberra Packard Central Europe GmBH). The graphical representation of the entrance of the treatment beam was aligned with the approximate location of the corpus callosum–hippocampus as determined from the pre-existing MRI and computed tomography (CT) scan of a rat. Thus, for evaluation of the dose distribution, the 90% and 70% isodose levels were superimposed on the image of the skull, aligned with the approximate location of the general rat brain structures (Figure 1A).

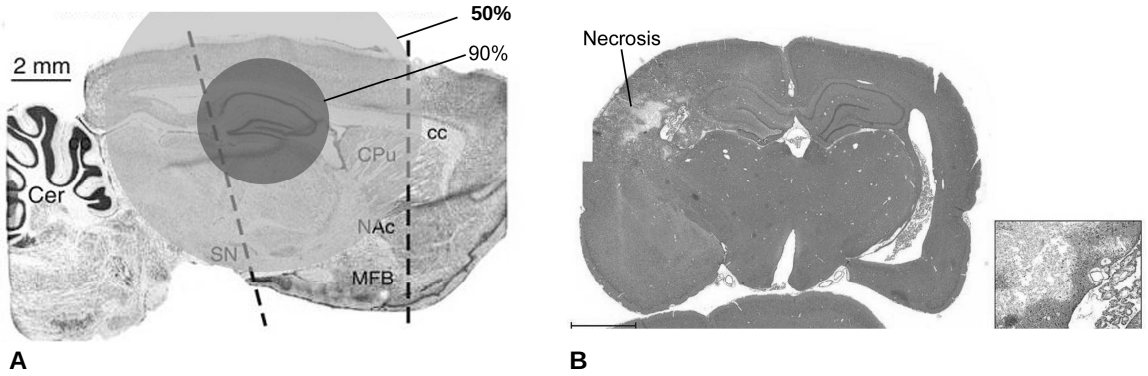

Figure 1. *Dose distribution using a 10 mm diameter beam. The 90% and 70% isodose levels are superimposed on the sagittal image of the rat brain (**A**). The haematoxylin–eosin (H&E) slide of the brain at the 70 Gy dose level. Damage caused by the irradiation on the left side localized to a defined small brain volume in the high-dose region, without any histopathological aberrations in the contralateral hemisphere (**B**). The sub-panel image right to image B shows the post-irradiation brain injury at higher magnification.*

III.5.3. Irradiation

Two prone adult male SPRD rats placed nose-to-nose in the irradiation position, with earpin fixation, were imaged in the Emotion 6 CT scanner (Siemens AG, Erlangen Germany) in order to obtain three-dimensional (3D) anatomical information for planning of the radiation geometry. Slices (1.25 mm) were obtained by using the maximum resolution afforded by the scanner. The whole brain, eyes, internal ears, corpus callosum and hippocampus on both sides, together with the target volume, were delineated in the XIO CMS™ treatment planning system (ELEKTA, Stockholm, Sweden), using MRI and the anatomy atlas of the rat brain. A 6 MeV lateral electron beam at a 100 cm

source-to-skin distance (SSD) was chosen because it has a sharp dose fall-off with depth, confining the radiation dose delivery to the defined volume of the hippocampus, including the corpus callosum of the ipsilateral hemisphere, while sparing the skin, the eyes, the ears, the cerebellum, the frontal lobe and the contralateral half of the brain (Figure 1A, 1B). No build-up bolus was used. The planned doses were delivered in a single fraction by means of a linear accelerator (Primus IMRT, Siemens, Erlangen, Germany) at a dose rate of 300–900 MU/min, with 6 circular apertures 10 mm in diameter, each in a 20 mm thick Newton metal insert placed into the 15 x 15 cm electron applicator, to the following groups of animals: 120 Gy (n=3), 110 Gy (n=3), 100 Gy (n=3), 90 Gy (n=6), 80 Gy (n=3), 70 Gy (n=6), 60 Gy (n=3), 50 Gy (n=6), 40 Gy (n=12) and sham-irradiated (n=12). Immediately prior to irradiation, the animals were anaesthetized with an i.p. injection of 4% chloral hydrate (1 ml/100 g Fluka Analytical, Buchs, Switzerland). They were placed 2-by-2, nose-to-nose, on the 3-storeyed positioning device on the couch of the irradiation unit and their heads were aligned individually at the intersection of the beam axis-marking lasers. The light field was directed at exactly the middle of the distance between the eye and ear, with the upper edge at the top of the skull. An ear plug was inserted into the ipsilateral ear. Pairs of animals were situated on all 3 storeys. The irradiation dose rate was 300/900 MU/min and de-escalated doses ranging from 120 to 40 Gy were applied, with 3–12 animals per dose level. The monitor units (3000 MU/10 Gy) used for the irradiation were derived from the previous small-field dosimetry. The radiation geometry was verified prior to the irradiation, and documented by control imaging on film after the irradiation (Figure 2). The animals were first imaged with the 6-hole insert exposed to 6 MeV electrons (50 MU), after which the insert was removed and a large field (20 x 20 cm) of 6 MeV photons was imaged (1.6 MU) to obtain an outline of the skull together with the body landmarks such as the oral cavity, ear canals, etc. Sham controls were anaesthetized, but not imaged or irradiated. Following treatment, the animals were transferred to their home cages and kept under standard conditions, with weekly weight measurements, descriptive behaviour observations and skin detection.

Figure 2. *The preparation for irradiation was performed by individual fixation of the rats after alignment of reference points under i.p. anaesthesia. Pairs of animals were situated on all 3 storeys*

of the positioning device. The radiation geometry was verified prior to the irradiation with the aid of the intersection of the beam axis-marking lasers, and documented by control imaging on film after the irradiation.

III.5.4. Magnetic resonance imaging

Sixty rats underwent 72 MRI procedures prior to or 4–19 weeks after irradiation. Randomly selected animals from each irradiation dose level were examined by means of 1.5 T MRI (Signa Excide HDxT, GE Healthcare, Little Chalfont, Buckinghamshire, UK), using a human head coil with a home-made styrofoam holder containing 6 animals under i.p. chloral hydrate (Sigma Aldrich, St Louis, MO, USA) anaesthesia. No contrast agent was used for the MRI images. Twelve animals underwent 3 MRI examinations, at baseline, at mid-term and prior to histology: coronal-T1 (T1: longitudinal relaxation time) 3D ultrafast gradient echo with magnetization preparation [IR-FSPGR], field of view [FOV] 17.0 mm^2, inversion time [TI] 450 slice thickness [ST]: 1.2 mm), sagittal (3D Cube T2, repetition time [Tr] 3000, echo time [TE] 60, FOV: 13 mm^2 , TI 450, ST: 1.2 mm, Space [Sp]: 0) and coronal T2 (T2: transverse relaxation time) weighted (3D IR-FSPGR; FOV: 13 mm^2 , ST: 1.2 mm, Sp: 0) images were acquired. The MRI procedure required about 10 min per sequence.

III.5.5. Histopathology

Rats were anaesthetized with 4% chloral hydrate and perfused transcardially with 0.1 M phosphate buffer solution (pH 7.0–7.4) before they were fixed with 4% paraformaldehyde buffer solution (pH 7.0–7.4) at 4 °C. The brains were dissected out and postfixed in paraformaldehyde for 1 day before being embedded in paraffin. Serial 30-μm-thick sections were cut with a vibratome. Sections were stained with H&E for histologic evaluation; for the demonstration of demyelination, Luxol fast blue staining was used. All analyses were performed blindly, using coded sections. Evaluations were carried out with a semiquantitative method, independently by 2 experienced histopathologists. A score was awarded for each examined parameter (necrosis, macrophage density, vascularization, haemorrhage, reactive gliosis, calcification and demyelination) on a semiquantitative scale of from 1 to 4 (where 1 represented the normal brain structure). In the case of necrosis, at low magnification (optical magnification [OM] 50x): 1: not detected; 2: necrosis detected in <50% of the examined field; 3: necrosis detected in 50–100% of the examined field; 4: the necrosis detected was larger than the FOV, or affected both hemispheres of the brain. The macrophage density was examined at high magnification (OM 400x): 1: no foamy macrophages detected; 2: 1–4 foamy macrophages/high-power field (HPF); 3: 5–10 macrophages/HPF; 4: >10 macrophages/HPF. Vascularization was scored (OM 50x) as 1: no neovascularization detected; 2: newly-formed small, simple capillaries

detected around the necrosis; 3: newly-formed capillaries detected around the necrosis, which contained variously-sized, but simple capillaries; 4: large, complex capillaries or small capillaries seen with endothelial proliferation. Haemorrhage (OM 50x): 1: no haemorrhage detected; 2: haemorrhage detected in a single, small focus; 3: haemorrhage seen in multiple small foci, or a single, larger focus; 4: extensive multiple haemorrhage detected. Reactive gliosis (OM 200x): 1: no; 2: mild; 3: moderate; 4: severe reactive gliosis detected in the brain.

Calcification (OM 50x): 1: no calcification; 2: a single small calcified focus detected; 3: multiple small or a single, larger focus detected; 4: extensive, multiple calcifications detected.

Demyelination (OM 400x): 1: none; 2: mild; 3: moderate demyelination, but fibres detected; 4: severe demyelination, with destruction of the fibres.

III.6. Application of GPC in the small-animal model of partial brain irradiation

III.6.1. Treatment

A total of 24 adult (6-week-old) male SPRD rats (purchased from the Animal House of the University of Szeged) were used in these experiments. The 40 Gy dose level (which was found to be appropriate for the detection of brain injury in a reasonable time period) was selected for the investigation of neuroprotection. Rats (weighing from 180 to 220 g) were anaesthetized (4% chloral hydrate (Fluka Analytical, Buchs, Switzerland), 1 ml/100 g, i.p.) and placed in the prone position, using laser alignment. After earpin fixation, they were imaged in the Emotion 6 CT scanner (Siemens AG, Erlangen, Germany) in order to plan the radiation geometry. The dosimetry of the small electron field and the method of irradiation were the same as previously. The following groups of animals participated in the experiment: a sham-irradiated control (CO) group (n=6), an only GPC-treated (GPC) group (n=6), an RT group (n=6), and a both GPC-treated and irradiated (GPC+RT) group (n=6). Beginning from 1 week before the day of irradiation, the rats received GPC (Lipoid GmbH, Ludwigshafen, Germany; 50 mg/kg bw, dissolved in 0.5 ml sterile saline, administered by gavage) or the vehicle at the same time every second day (on Mondays, Wednesdays and Fridays) for 4 months.

III.6.2. Histopathology

The preparation for and conductance of the histopathology were the same as reported above. Sections were analysed under an Axio Imager.Z1 (EC Plan Neofluar 40x/0.75 M27, Freiburg, Germany) light microscope, and photomicrographs were taken with AxioCam MR5 camera equipment. Digital photos were analysed with the aid of Image-Pro® Plus 6.1 software

(MediaCybernetics Inc., Bethesda, MD, USA). All analyses were carried out blindly on coded sections by 2 independent histopathologists. The examined parameters and the scoring system were not altered.

III.7. Statistical analysis

All statistical analyses of HPLC measurements were performed with the help of the SPSS Statistics 17.0 software. We first checked the distribution of data populations with the Shapiro-Wilk W test. All the data of the experimental groups exhibited Gaussian distribution. We then performed the Levene test for analysis of the homogeneity of variances. The 4 groups in each set of the 4 experiments were compared by using one-way measures of analysis of variance (ANOVA) followed by a Bonferroni *post hoc* test comparison when equal variances were assumed, or by a Games-Howell *post hoc* test comparison when equal variances were not assumed. The null hypothesis was rejected when the p level was <0.05, and in such cases the differences were considered significant. Data were plotted as means (+ standard error of the mean (SEM)) in the graphs.

For statistical evaluation of the data in the behavioural tests and histopathology, one-way ANOVA was used, followed by Fisher's LSD *post hoc* test with StatView 4.53 for Windows software (Abacus Concept Inc., Berkeley, CA, USA). These data were expressed as means+SEM. Levels of statistical significance in the behavioural tests were taken as $p \leq 0.05$ and $p \leq 0.01$.

Measurement of the level of agreement between the two independent histopathologists was performed in R Version 3.0.2 with the Cohen κ-test for the different items used to assess the morphological changes after partial brain irradiation. This measure calculates the degree of agreement in classification over that which would be expected by chance and is scored as a number between 0 and 1. A κ value of ≥ 0.8 indicates excellent, 0.6–0.8 good, 0.4–0.6 moderate, 0.2–0.4 poor, and <0.2 no agreement. All p values were corrected according to Bonferroni and were considered statistically significant if $p<0.05$.

IV. RESULTS

IV.1. Detection of catecholamines

We first tested the effects of pre- and post-treatment with SIL on the MPTP-induced significant changes in striatal DA ([$F_{(3,29)}$=10.074, p<0.001, Games-Howell *post hoc* test: p<0.05]; Figure 3A), DOPAC ([$F_{(3,29)}$=5.45, p<0.05, Bonferroni *post hoc* test: p<0.05]; Figure 3B) and HVA levels ([$F_{(3,29)}$=7.817, p<0.001, Bonferroni *post hoc* test: p<0.05]; Figure 3C). The SIL treatment did not influence these alterations appreciably. In the second set of experiments, we tested the effects of pre- and post-treatment with NGN on MPTP toxicity. In this set of experiments, although the NGN treatment did not significantly alter the reductions caused in the striatal DA ([$F_{(3,24)}$=9.552, p<0.001, Games-Howell *post hoc* test: p<0.05]; Figure 3D) and DOPAC ([$F_{(3,24)}$=10.908, p<0.001, Bonferroni *post hoc* test: p<0.01]; Figure 3E) levels by MPTP administration, a slight lessening of the DA decrease was observed. In this experiment, the HVA levels were not altered significantly at all (Figure 3F). In the third set of experiments, we tested the effects of pre- and post-treatment with SP on the significant MPTP-induced reductions in striatal DA ([$F_{(3,26)}$=98.189, p<0.001, Bonferroni *post hoc* test: p<0.001]; Figure 3G), DOPAC ([$F_{(3,26)}$=36.75, p<0.001, Bonferroni *post hoc* test: p<0.001]; Figure 3H) and HVA ([$F_{(3,26)}$=26.95, p<0.001, Games-Howell *post hoc* test: p<0.001]; Figure 3I) levels. The SP treatment did not influence the MPTP-induced changes, but slightly increased the MPTP-caused lethality in mice: 1 of the 10 mice died in the MPTP-treated group, whereas 3 died in the SP- and MPTP-co-treated group. In the last set of experiments, we tested the effects of pre- and post-treatment with AP on MPTP toxicity. In this set of experiments, MPTP administration caused significant reductions in the striatal DA ([$F_{(3,23)}$=52.339, p<0.001, Games-Howell *post hoc* test: p<0.001]; Figure 3J), DOPAC ([$F_{(3,23)}$=42.98, p<0.001, Bonferroni *post hoc* test: p<0.001]; Figure 3K) and HVA ([$F_{(3,23)}$=24.54, p<0.001]; Figure 3L) levels as compared with the CO values. Although the AP treatment did not influence the MPTP-induced changes significantly, it considerably increased the MPTP-caused lethality in mice, as 1 of the 10 mice died in each of the AP- and MPTP-treated groups, whereas 7 died in the AP- and MPTP-co-treated group. It is also important to mention that none of the tested compounds themselves altered the CO levels of DA, DOPAC and HVA.

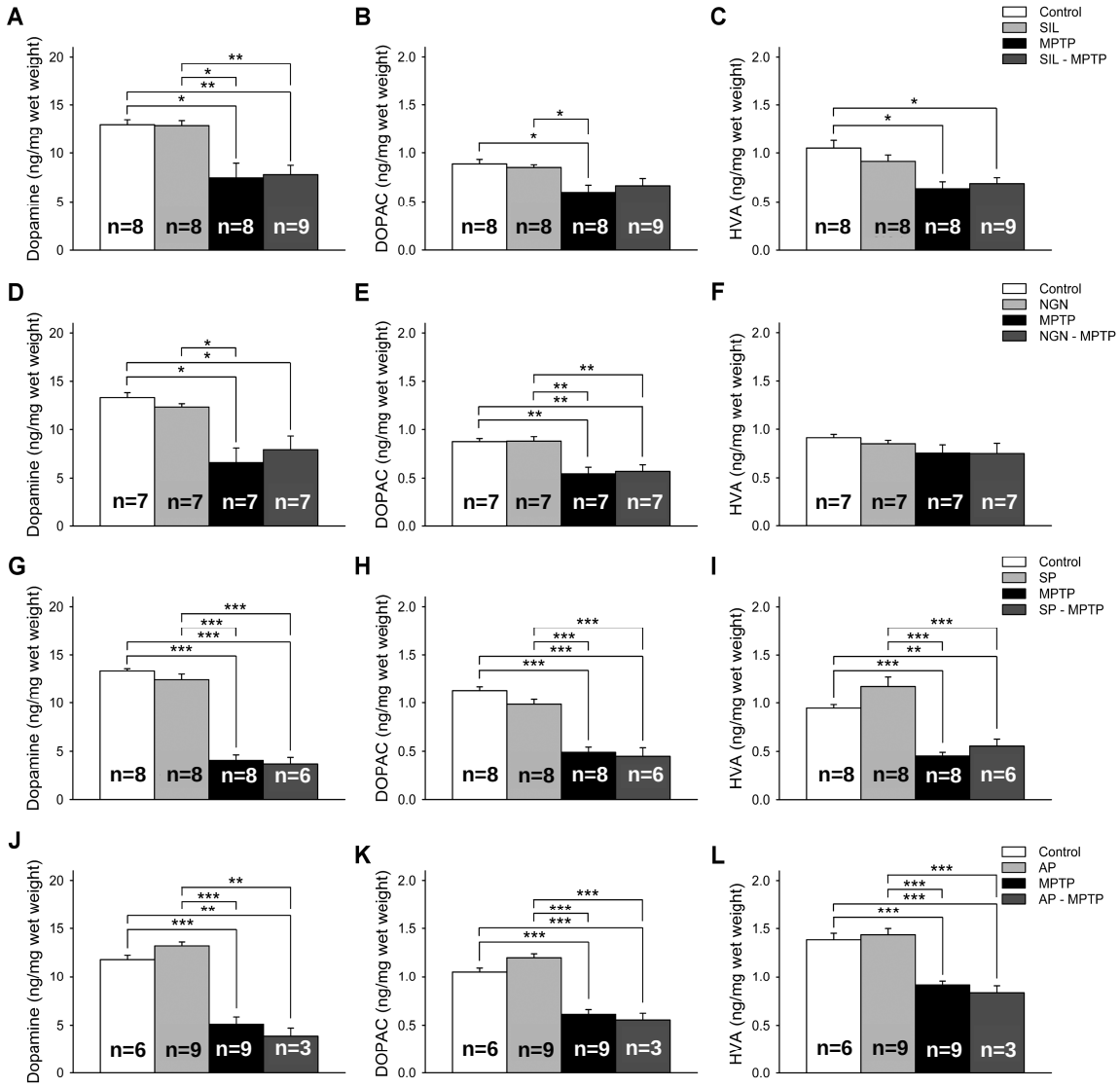

Figure 3. *The effects of SIL, NGN, SP and AP treatments on the MPTP-induced decreases in striatal DA, DOPAC and HVA concentrations in C57B/6 mice. The treatment with SIL apparently did not affect the MPTP-induced reductions in striatal DA (**A**) and HVA (**C**) levels, while it abolished the significant decrease in DOPAC (**B**) level. Although NGN treatment slightly, but not significantly attenuated the MPTP-induced reduction in striatal DA level (**D**), it did not alter the change in DOPAC level (**E**), and no significant change in HVA level (**F**) was observed. SP did not affect the MPTP-induced reduction in striatal DA (**G**), DOPAC (**H**) or HVA (**I**) levels. AP did not alter the MPTP-induced decreases in striatal DA (**J**), DOPAC (**K**) and HVA (**L**) levels. Data are means+SEM; *p<0.05, **p<0.01, ***p<0.001.*

IV.2. Behavioural performances of animals treated with KYNA analogues

Four of the newly synthetized KYNA amides were further investigated in behavioural experiments. Open-field observations were made on 5 groups of animals: a CO group (injected with saline), and KYNA-1, KYNA-2, KYNA-6 or KYNA-11-treated groups. These analogues were chosen for the following reasons: KYNA-1 was the only new amide that proved effective as an inhibitor in a previous *in vitro* study, KYNA-2 is structurally very similar to KYNA-1, differing only in containing an additional $–CH_2–$ group in the side-chain; KYNA-6 and KYNA-11 (KYNA-11, L-KYN sulphate, was tested earlier by Gigler et al. 2007; Németh et al. 2004) differ appreciably in structure not only from each other, but also from KYNA-1 and KYNA-2.

In acute behavioural experiments, the animals were treated with saline (CO) or KYNA amide analogue 2 h prior to the behavioural observations, while chronic treatment was administered on 9 successive days, with observations on day 9, 2 h after the final injection. The animals treated with one or other KYNA amide analogue did not differ greatly in behaviour from those that received the saline vehicle. The posture and activity were quite similar in each group. The ambulation time, the mean velocity and the number of rearings did not exhibit highly significant differences in most cases (Figure 4). Although the ambulation time was somewhat decreased after KYNA-11 administration, the changes were not significant (Figure 4A). The mean velocities were nearly the same in each group (Figure 4B). Significant changes in performance were observed only in the numbers of rearings. Both KYNA-1 and KYNA-11 decreased the number of rearings in the acute experiments, and KYNA-11 did so in the chronic experiments too (mean+SEM, $p<0.05$, $p<0.01$; Figure 4C). Similar behavioural observations were made on rats, but those results are not detailed here.

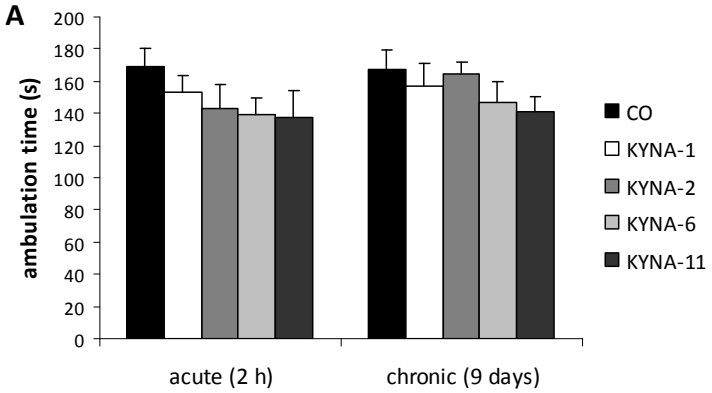

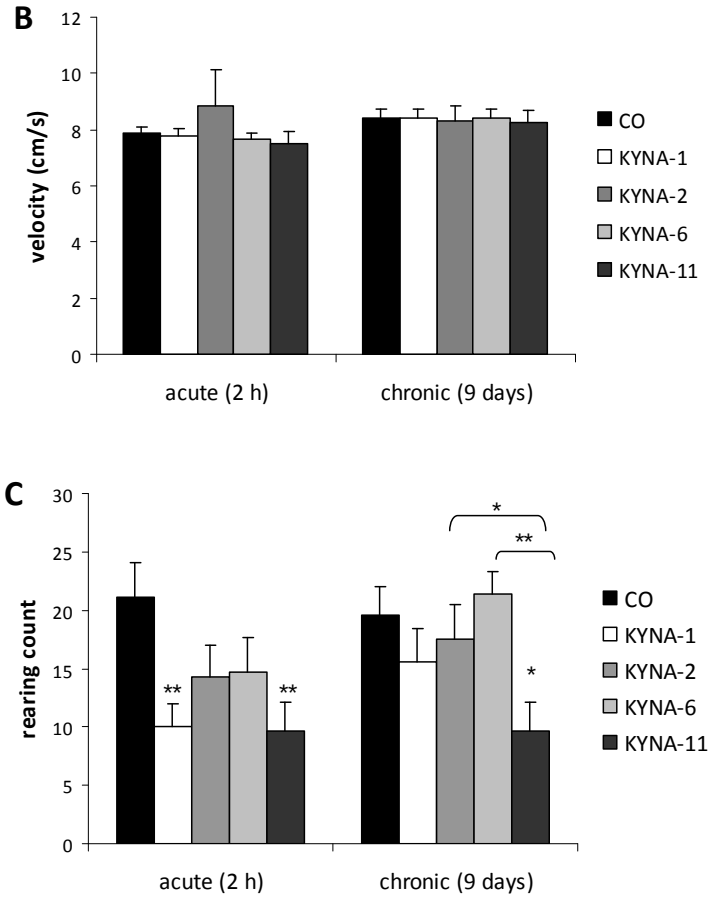

Figure 4. *Observations in the open-field arena. (**A**) Time spent in ambulation. No difference was found between the CO and treated groups in either the acute or the chronic experiments. (**B**) Velocity of the movements of the mice. No difference was found between the CO and treated groups in either the acute or the chronic experiments. (**C**) Number of rearings during 5-min observation periods. KYNA-1 and KYNA-11 significantly reduced the number of rearings in the acute experiments, as did KYNA-11 in the chronic experiments (mean+SEM; *p<0.05, **p<0.01). If not labelled, the comparisons were made with the CO group.*

IV.3. Results of small-animal irradiation

The morphological and functional changes were evaluated at dose levels in the range 90–40 Gy: outside this dose range, either lethal or serious events (120–100 Gy) or no changes (doses <30 Gy; data not reported here) occured during the at most 4-month post-irradiation follow-up period.

At the highest dose (120 Gy), all of the animals underwent a rapid severe general and neurofunctional decline (Figure 5) and died or had to be euthanized between 25 and 40 days after the irradiation. The rats irradiated at the 110 Gy dose level survived longer, but also deteriorated between 30 and 50 days post-irradiation. At the lower dose levels, there were no signs of a general

impairment; the weight gain, eating habits and daily activity did not differ from those of the control rats. All the RT animals suffered hair loss from the site corresponding to the beam entrance within 30 days following the irradiation.

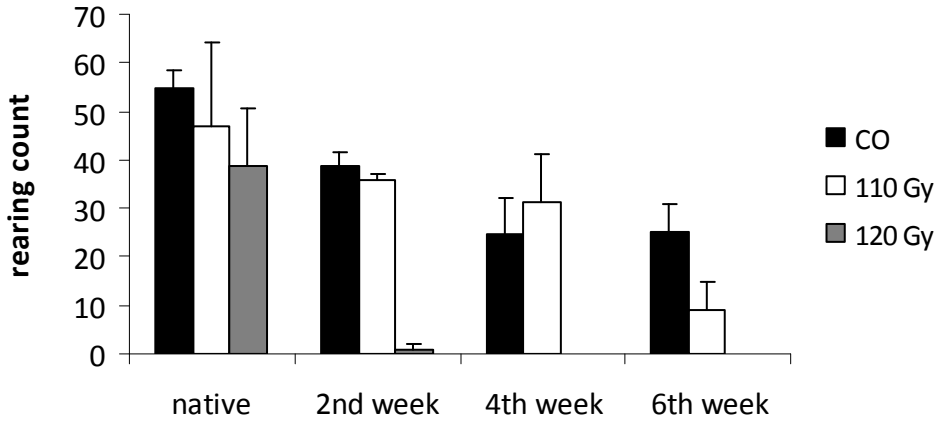

Figure 5. *The explorative behaviour of the animals began to diminish 2 weeks after irradiation at the 120–110 Gy dose levels, but the rats died before marked changes could occur in this parameter (mean+SEM).*

IV.3.1. Neurofunctional observations

In the early monitoring, significant differences in the spontaneous locomotor activity of the rats irradiated at 90–40 Gy were not detected with the open-field test (neither in the ambulation time nor in the mean velocity), but the motor function began to decline slightly 8 weeks after irradiation with the 90 Gy dose. The rearing count was significantly reduced in the groups that received 90–60 Gy. The time at which the rearing activity started to diminish was dose-dependent: It was 40–55 days post-irradiation after the 90 Gy dose (mean+SEM, $p<0.05$) (Figure 6). The animals that received 120 Gy died before marked changes could be seen in this parameter.

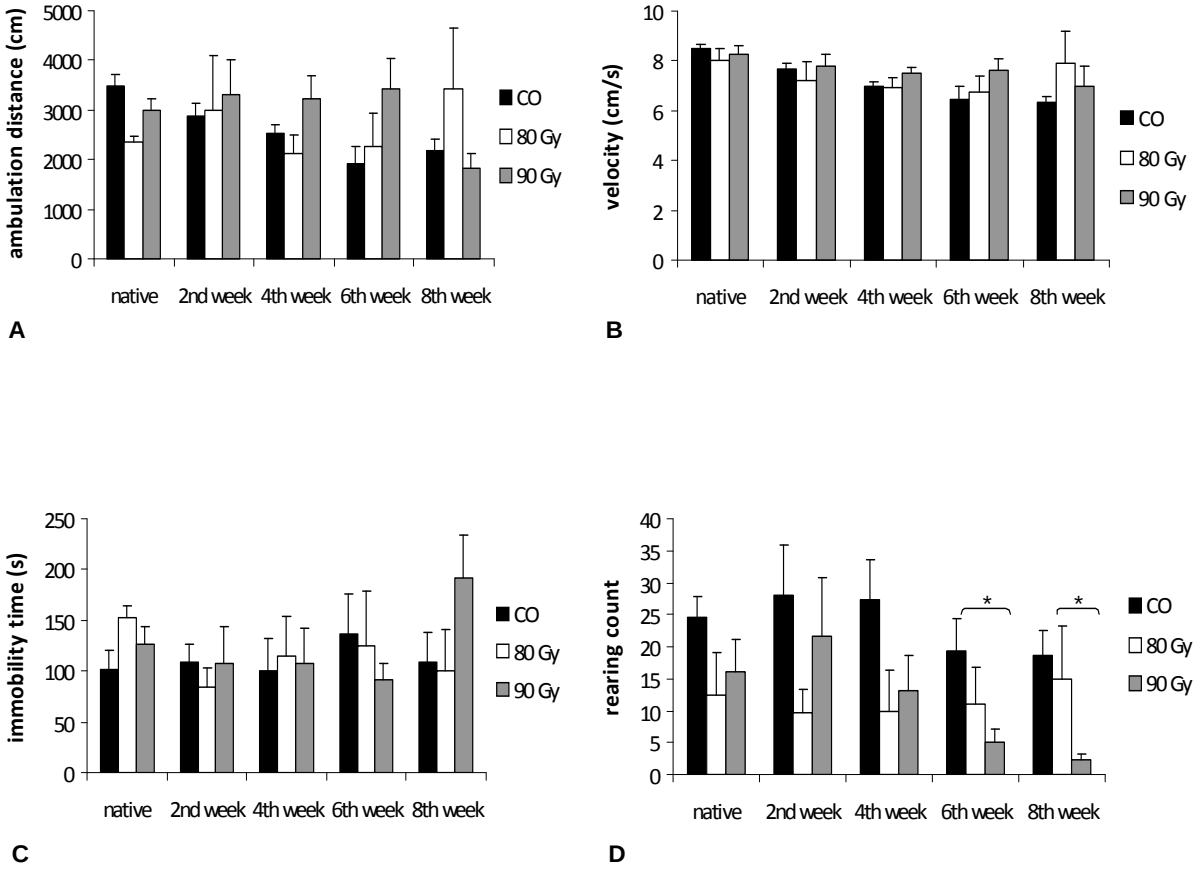

Figure 6. *At the 90 Gy dose level, interesting changes in ambulation ability were detected after 6 and 8 weeks. The number of rearings also decreased in the 90 Gy group relative to the CO. The mean velocity and the immobility time of the rats did not change markedly (mean+SEM; *p<0.05).*

The MWM test was found to be a highly sensitive tool for the detection of a neurofunctional impairment. A relevant memory deterioration was detected soon after the dose delivery at the 70 Gy dose level and the difference increased with time ($p<0.001$). A significant cognitive deficit was also observed 8 weeks after the irradiation in the group treated with 60 Gy (mean+SEM, $p<0.05$) (Figure 7).

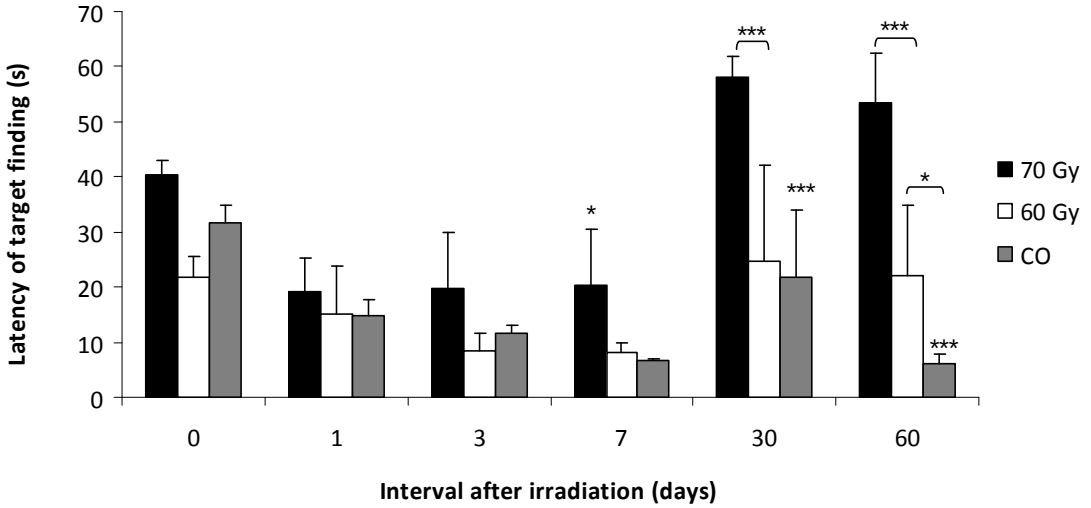

Figure 7. *Memory deterioration was detected 7 days after the dose delivery at the 70 Gy dose level and the difference increased with time (mean+SEM; *p<0.05, ***p<0.001). At the 60 Gy dose level, a significant cognitive deficit was observed 8 weeks after the irradiation (mean+SEM; *p<0.05).*

The commencement of the impairment of the learning-memory function proved to be dose-dependent; in the groups irradiated at 50–40 Gy, the first sign of deterioration was detected 30 days post-irradiation and the difference relative to the CO animals was more pronounced after 90 days (Figure 8).

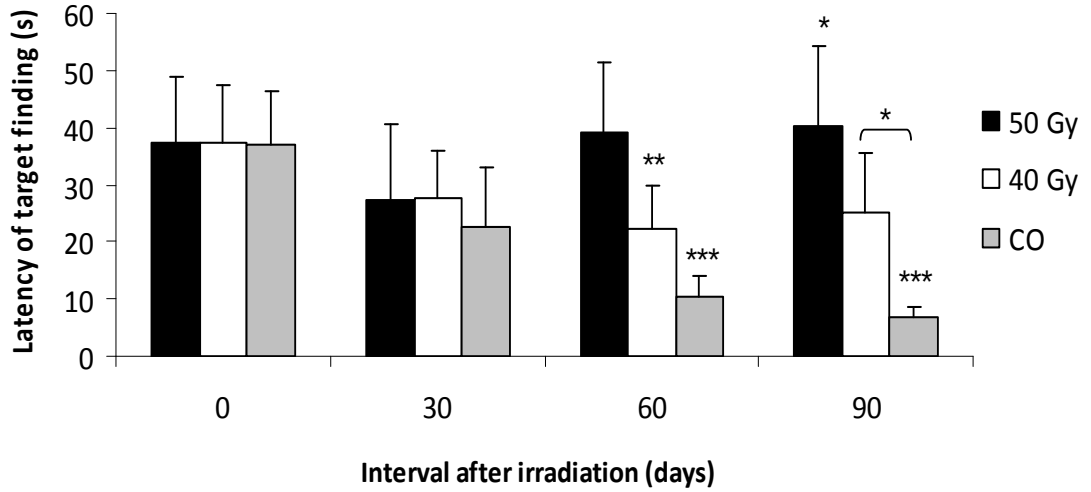

Figure 8. *In the groups irradiated at 50–40 Gy, the first sign of deterioration was detected 30 days post-irradiation and the difference relative to the CO animals was more pronounced after 90 days (mean+SEM; ***p<0.001).*

IV.3.2. MRI findings

Serial MRI records demonstrated structural damage in the form of cavity formation in the cortical region, with extensive perifocal oedema, which generally appeared 2–4 months following irradiation (Figure 9). We performed the first post-irradiation MRI after 4 weeks in the majority of the cases, since our aim was to investigate late effects.

120 Gy resulted in a serious deterioration within 4 weeks in all rats. Localized radiation-induced cystic necrosis began to appear at approximately 4–8 weeks post-irradiation in one hemisphere of rats irradiated with 120–60 Gy; after a lower dose, the structural changes emerged later, 19–24 weeks after irradiation, in the T1 and T2-weighted (T2W) images of the ipsilateral hemisphere, in both the coronal and the sagittal plane (Figure 10).

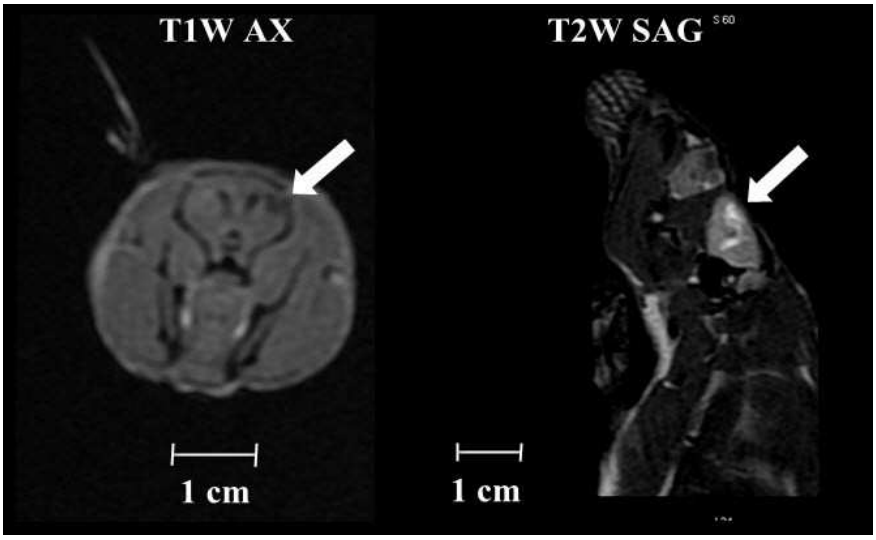

Figure 9. *MRI revealed visible structural damage in the form of cavity formation in the cortical region, with extensive perifocal oedema, which appeared from 2 to 4 months following irradiation. Arrows show the site of the radiation injury. T1W AX: the T1-weighted image of the brain in the axial plane; T2W SAG: the T2-weighted image of the brain in the sagittal plane.*

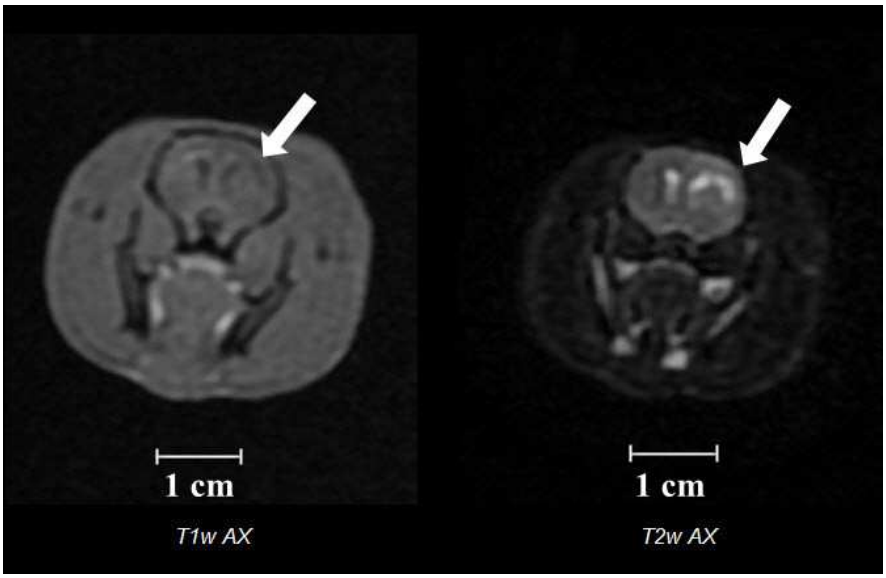

Figure 10. *Radiation-induced cystic necrosis began to appear at 4–8 weeks post-irradiation in rats irradiated with 120–60 Gy; at lower doses, the structural changes were observed later, 19–24 weeks after irradiation, in the T1W and T2W images, in the ipsilateral hemisphere in the coronal plane. Arrows show the sites of radiation injury.*

IV.3.3. Histopathological evaluations

No signs of necrosis, i.e. neither reactive gliosis nor any of the other examined histopathological categories, were seen on the H&E-stained slides of the CO animals and the non-irradiated regions of the brain of the RT animals (Figure 1B). The following parameters correlated closely with the high (120–90 Gy), medium (80–60 Gy) or low dose (50–40 Gy) level in the irradiated region of the brain: reactive gliosis, vascularization, macrophage density, necrosis and calcification. No significant dose dependence was detected as concerns the extent of haemorrhage (Figure 11D). The dose >90 Gy groups displayed severe necrosis that reached the grey and white matter, causing severe demyelination, with destruction of the fibres. The levels of necrosis, reactive astrogliosis and calcification and the density of the foamy macrophages were markedly elevated in these groups as compared with the CO animals (Figure 11).

The extent of the haemorrhage was significantly higher than for the other RT animal groups. The scores in the 90 Gy group were as follows: necrosis (2.83), macrophage density (2.33), neovascularization (2.50), haemorrhage (1.0), reactive astrogliosis (2.0), calcification (2.17) and demyelination (3.0). Severe-to-moderate necrosis was seen in the 80–60 Gy groups, with severe-to-moderate demyelination, but the fibres could mostly be detected. In comparison with the control group, significant correlations were detected in the following categories: necrosis, macrophage

density, vascularization, calcification and reactive gliosis. Moderate haemorrhage was observed in the animals irradiated with the 80 Gy dose. The scores were as follows: necrosis (1.89), macrophage density (2.00), neovascularization (1.89), haemorrhage (1.1), reactive astrogliosis (1.3), calcification (1.3) and demyelination (2.2). In the 50–40 Gy groups, mild-to-moderate necrosis was detected, with mild-to-moderate demyelination. Significantly increased levels of necrosis, vascularization and reactive astrogliosis were seen. Mild calcification occurred. Interestingly, in 1 animal irradiated with the 50 Gy dose, meningoencephalitis was observed, but the presence of bacteria was not seen. The scores were as follows: necrosis (1.45), macrophage density (1.00), neovascularization (1.00), haemorrhage (0.73), reactive astrogliosis (0.73), calcification (0.91) and demyelination (1.27).

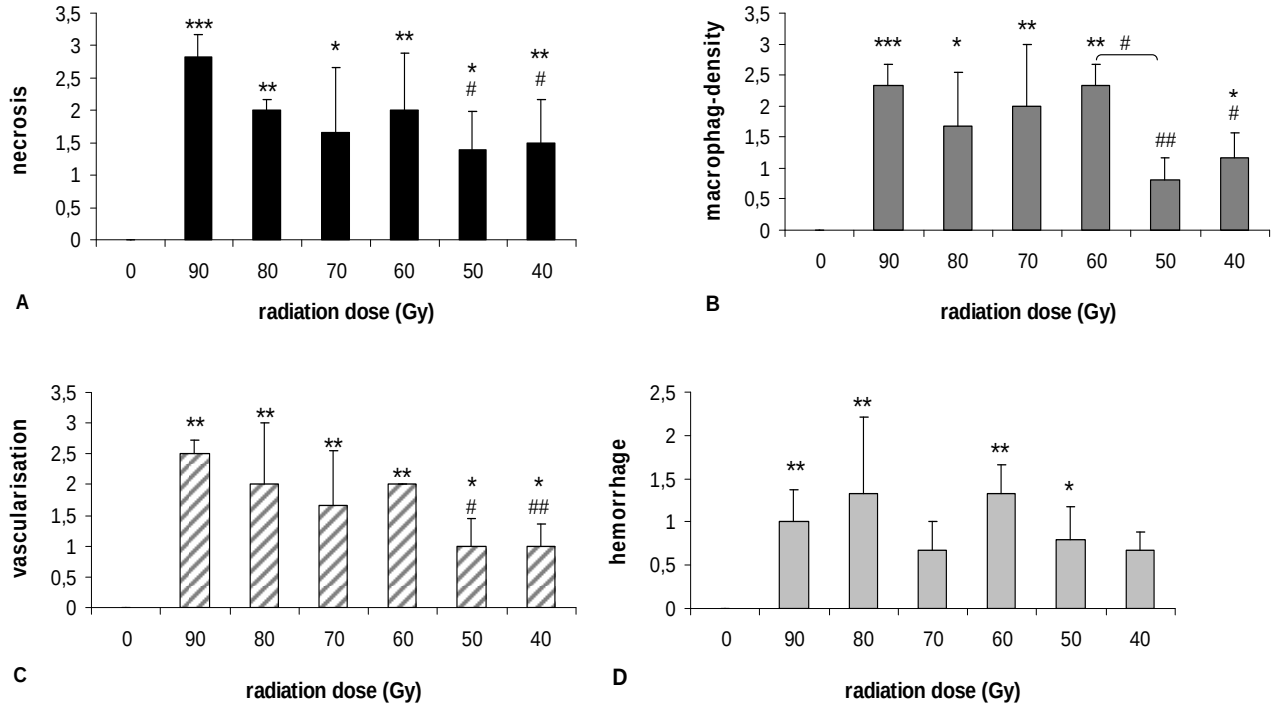

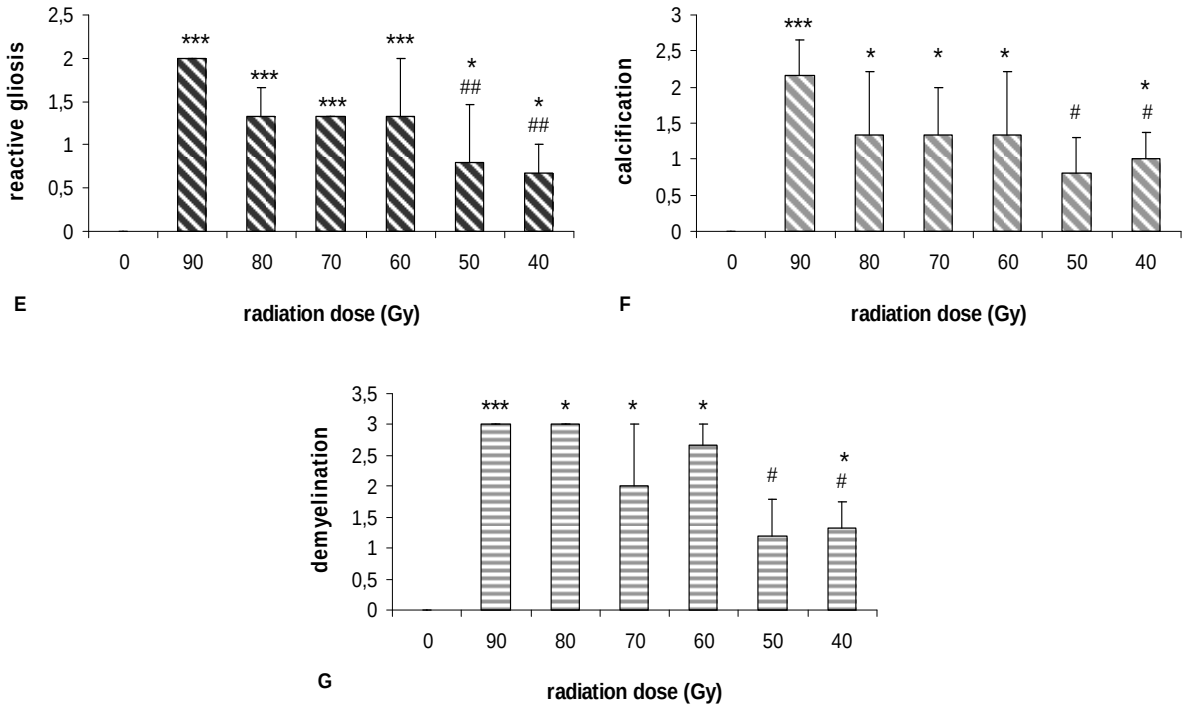

Figure 11. *Dose-related histopathological changes after partial brain irradiation. In the RT region of the brain, the degree of necrosis correlated closely with the dose level (mean+SEM, n_{co}=15, n_{40Gy}=6, n_{50Gy}=4, n_{60Gy}=3, n_{70Gy}=6, n_{80Gy}=3, n_{90Gy}=6). n_{co}=number of CO rats, n_{xGy}=number of rats irradiated at the x Gy dose level. The significance level between the CO and RT groups is indicated by *; and the significance level between the 90 Gy group and the remaining RT groups by $^{\#}$ (**A**). The numbers of foamy macrophages (**B**) were significantly elevated relative to the CO animals in all groups. A significant correlation was detected in the degree of vascularization in the RT volume between the CO and the 90 Gy group (**C**). Relative to the CO group, the level of haemorrhage was significantly increased in all groups except those that received 70 Gy or 40 Gy (**D**). The degree of reactive gliosis was significantly elevated in all the RT groups compared to the CO animals (**E**). A significant correlation was detected in the degree of calcification in the RT volume between the CO and the groups irradiated at the 120–90 Gy, 80–60 Gy and 50–40 Gy dose levels (**F**). The higher doses caused severe demyelination, with destruction of the fibres, and the intermediate doses led to severe-to-moderate demyelination, while the lower doses resulted in only mild-to-moderate demyelination (**G**).* $^{\#}p<0.05$; $^{*}p<0.05$; $^{\#\#}p<0.01$; $^{**}p<0.01$; $^{\#\#\#}p<0.001$; $^{***}p<0.001$.

IV.4. Treatment with GPC

The 40 Gy RT group exhibited a body weight deficit; their body weight remaining under the normal throughout. The difference between the RT and CO groups did not reach the level of statistical significance.

IV.4.1. MWM test

The MWM test was used to assess the acquisition and retention of a spatial working memory. Healthy rats improve their performance during such place navigation by using their spatial working memory. After the 40 Gy irradiation, significant, time-related changes in learning ability were detected in both the RT and GPC+RT groups, but these changes were significantly reduced in the GPC+RT group (Figure 12). The first sign of deterioration was detected 90 days post-irradiation and the difference relative to the CO animals was more pronounced after 120 days ($p<0.001$). A relevant memory impairment was detected in the RT group after 120 days, and a significant cognitive deficit was also observed in the GPC+RT group relative to the CO group ($p=0.0025$). Despite this, there was a significant amelioration after GPC management, which reduced the latency of target finding relative to the RT group ($p=0.012$). The GPC ameliorated the memory of the animals and shortened the latency time of platform finding.

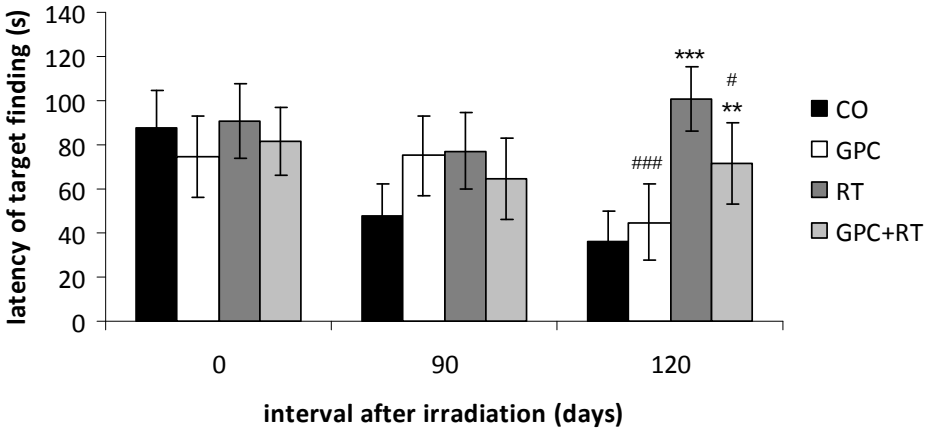

Figure 12. *Latency of target finding during the MWM test (mean±SEM). Pretreatment with GPC decreased the latency time after irradiation, the GPC+RT animals displaying a similar performance to that of the CO and GPC groups. The decrease on day 120 was significant ($p=0.012$). The symbol * indicates a significant difference relative to the saline-treated CO group, and the symbol # a significant difference relative to the RT group.* $^{\#}p<0.05$; $^{**}p<0.01$; $^{\#\#\#}p<0.001$; $^{***}p<0.001$.

IV.4.2. Histopathology

The H&E-stained slides of the CO animals and the non-irradiated regions of the brain of the treated animals exhibited no signs of necrosis, i.e. neither reactive astrogliosis, nor any of the other examined histopathological categories. In the irradiated region of the brain, the following parameters correlated closely with the 40 Gy dose level: necrosis, macrophage density, reactive gliosis, calcification and demyelination. The RT group displayed moderate necrosis that reached the grey

and white matter, causing demyelination, with destruction of the fibres. The grades of reactive astrogliosis and calcification, the density of the foamy macrophages and the degree of demyelination were all significantly elevated in the RT group as compared with the CO animals. Marked protective effects of GPC were detected as concerns the macrophage density ($p<0.001$), reactive astrogliosis ($p<0.001$), calcification ($p=0.012$) and the extent of demyelination ($p=0.035$). The scores in the RT group were as follows: necrosis 3.33, macrophage density 2.83, reactive astrogliosis 3.50, calcification 3.0 and demyelination 3.17. In the GPC+RT group, mild-to-moderate necrosis was seen, with mild-to-moderate demyelination, but the fibres could mostly be detected. In comparison with the CO group, significant correlations were detected in the following categories: necrosis, macrophage density, reactive gliosis, calcification (Figure 13) and demyelination (Figure 14). The scores were as follows: necrosis 2.33, macrophage density 1.50, reactive astrogliosis 1.83, calcification 2.0 and demyelination 2.17 (Figure 15).

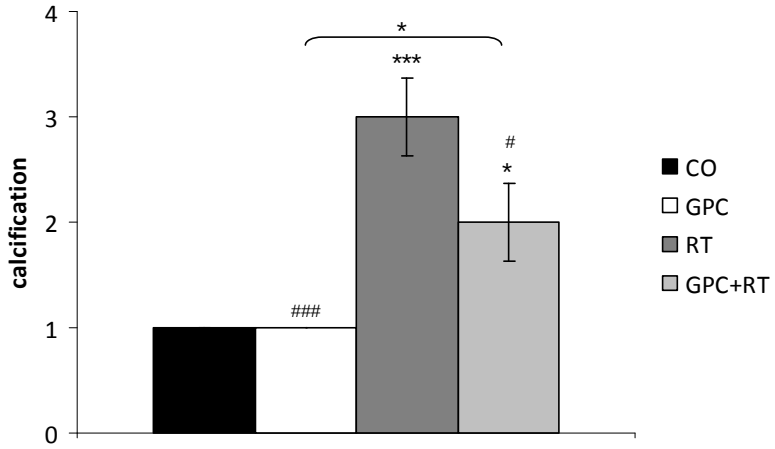

Figure 13. *As expected, the degree of calcification after 120 days was markedly higher in the RT group than in the CO group, and the GPC treatment protected the brain tissue from this effect (mean±SEM, p=0.013). The symbol * indicates a significant difference between the CO and RT groups; and the symbol # indicates a significant difference between the RT and the other groups.* $^{\#}p<0.05$; $^{*}p<0.05$; $^{\#\#\#}p<0.001$; $^{***}p<0.001$.

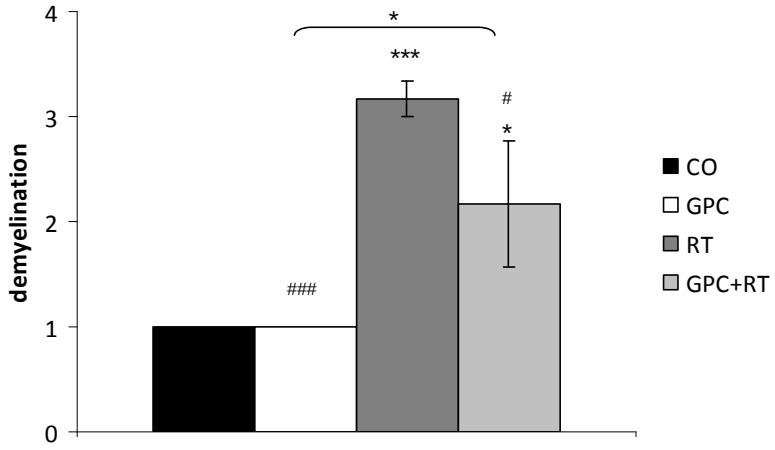

Figure 14. *The level of demyelination after 120 days was significantly higher in the RT group as compared with the CO animals, while GPC exerted a marked protective effect (mean±SEM, p=0.034). The score in the RT group was 3.17. In the GPC+RT group, mild-to-moderate demyelination was seen, but the fibres could mostly be detected. The symbol * indicates a significant difference between the CO and RT groups; and the symbol # indicates a significant difference between the RT and the other groups.* $^{\#}p<0.05$; $^{*}p<0.05$; $^{\#\#\#}p<0.001$; $^{***}p<0.001$.

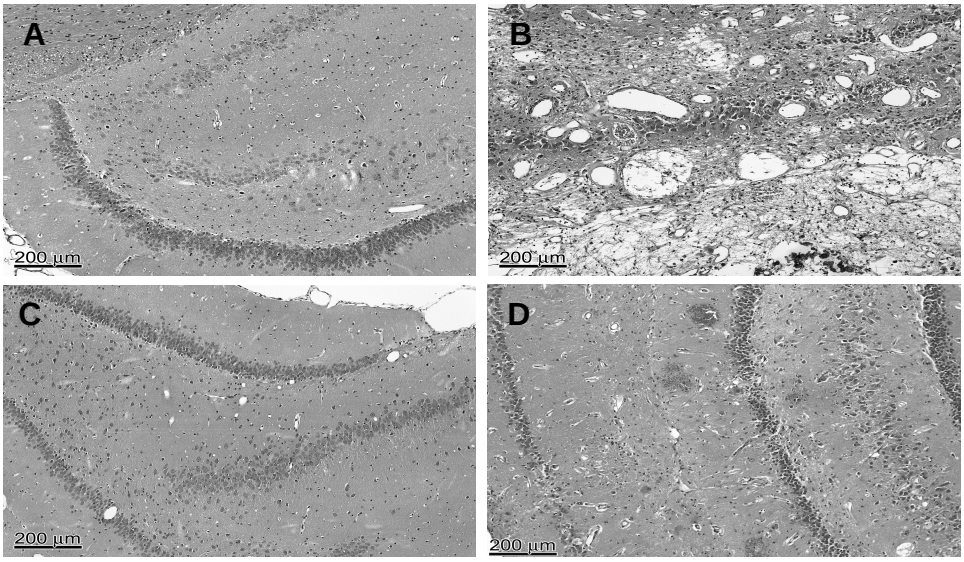

Figure 15. *Light micrographs of the hippocampal region in the non-irradiated CO group of rats. Histopathological changes of the hippocampus in response to irradiation and administration of GPC (**A**). RT group: severe necrosis that reached the grey and white matter, causing demyelination, with destruction of the fibres (**B**). The GPC-treated group was similar to the sham-irradiated group (**C**). In the GPC+RT group, marked protective effects of GPC were detected as concerns the macrophage density, reactive astrogliosis, calcification and the extent of demyelination. Only focal haemorrhage was noted (**D**). Scale bar: 200 µm.*

V. DISCUSSION

The role of MRPs in the MPTP-induced neurotoxicity

There is increasing evidence supporting the roles of BBB and BCSFB dysfunctions in neurodegeneration, including PD. Although the alteration in P-gp-mediated transport has been demonstrated to play a central role in the neurodegenerative process (Drozdzik et al. 2003), only a few data are available on the involvement of MRPs in PD. The aim of our study was therefore to assess the effects of certain compounds which can modulate the function of MRPs expressed on the BBB and BCSFB (MRP1, 2, 4 and 5) on MPTP toxicity in C57B/6 mice. Two of these compounds, SIL and NGN, are well-known flavonoids (most of these compounds have potent antioxidant and free radical scavenging properties) (Ross & Kasum 2002), which have already been tested in certain toxin models of PD, but not in the MPTP model. SIL, which is known to exert complex pharmacological action (Saller et al. 2007) including MRP inhibitor properties, is capable of the attenuation of maneb- and paraquat-induced lipid peroxidation (Singhal et al. 2011). However, in our study SIL did not alter MPTP-induced neurotoxicity. The reason for this difference would be that maneb and paraquat were applied in a chronic treatment regime twice a week for 9 weeks, which presumably caused less harm than that in the widely applied acute MPTP model. The other flavonoid, NGN, with MRP1, MRP2 and MRP4 stimulator properties, was moderately protective against 6-hydroxy-DA-induced neurotoxicity as it significantly attenuated the loss of DAergic neurones and the decrease in striatal DA levels (Zbarsky et al. 2005). Accordingly, in our study NGN treatment caused a slight, but not significant preservation of striatal DA content. In contrast with the above flavonoids, the effects of SP have not been tested in toxin models of PD. Although it did not appear to affect the striatal DA concentrations in our study, it slightly increased the MPTP-caused lethality in C57B/6 mice. It should be mentioned here that SP can reduce serum urate levels through its uricosuric effect. In a previous study, oral high-dose administration of the xanthine oxidase inhibitor and MRP4 stimulator AP resulted in a decreased level of urate, which may have an important role in the neuronal antioxidant pool in the striatum, but did not affect the DA level in rats (Miele et al. 1995; Desole et al. 1996). Accordingly, in our study AP considerably enhanced the MPTP-caused lethality, but the striatal DA content was preserved in the survivors. The main explanation for the potentiation of MPTP toxicity by AP would be the decrease of urate concentration by the inhibition of xanthine oxidase. However, an enhanced transport by MRP4 would also accompany the depletion of urate. Hence, a decrease in serum urate level would accompany the progression of PD (Sun et al. 2012).

The depletion of striatal urate by AP (which could be enhanced by its MRP4 stimulatory effect) or the use of probenecid (with MRP1 and 5 and organic acid transporter inhibitory and uricosuric effects) clearly augmented MPTP toxicity in C57B/6 mice, while SP (with MRP1, 4 and 5 inhibitory, MRP2 stimulatory and uricosuric effects) only slightly augmented MPTP-induced neurotoxicity. On the other hand, a mild level of prevention of the DA decrease was observed in mice treated with one flavonoid, NGN (with MRP1, 2 and 4 stimulatory effects), but no influence by another flavonoid, SIL (with MRP1, 2, 4 and 5 inhibitory effects). In conclusion, these data indicate that the depletion of urate augmented by MRP4 stimulation increases, while the stimulation of MRP1- or 2-mediated transporters (probably GSH-conjugated toxic substances) slightly attenuated MPTP-induced neurotoxicity.

Effects of some KYNA analogues

It was important that KYNA-1, which had proved neuroprotective in several models (Vámos et al. 2009; Marosi et al. 2010; Németh et al. 2006; Knyihar-Csillik et al. 2008), and partially inhibited NMDA-mediated synaptical transmission in the hippocampus, did not induce significant changes in the behaviour of the tested animals. The results confirmed that none of the studied KYNA derivatives induced major changes in the behaviour of these animals. Only the number of rearings was reduced somewhat after KYNA-1 or KYNA-11 administration. Moreover, as KYNA-1 did not significantly influence the behavioural performance in the open-field arena, KYNA-1 treatment does not appear to have any appreciable side-effects.

Focal rat brain irradiation model

A simple and effective method was developed for the delivery of a radiation dose to a well-defined area in one hemisphere of the brain, including the hippocampus and corpus callosum, in rats, similarly to human brain tumour radiotherapy, as recommended by others (Kalm et al 2013). It allows the investigation of a maximum of 6 small animals simultaneously and comprises a reproducible experimental model for quantification of the functional and morphological changes occurring due to radiation-induced focal brain damage within a reasonable time frame. Preclinical studies on CNS injuries have mainly made use of non-targeted dose delivery resulting from whole-body radiation fields with the selective shielding of extracranial parts (Akiyama et al. 2001, Vinchon-Petit et al. 2010), or whole-brain irradiation using a standard field with a bolus above the skull (Ernst-Stecken et al. 2007). However, highly selective dose delivery techniques were recently introduced for humans in the cases of head and neck and primary brain tumours. For radiobiological investigations in an experimental setting corresponding to clinical radiotherapy, conformal partial

brain irradiation has been performed on large animals (Tiller-Borcich et al. 1987, Lunsford et al. 1990, Yamaguchi et al. 1991, Spiegelmann et al. 1993), or a sophisticated technique, such as small animal stereotactic irradiation either with a gamma knife (Yang et al. 2000, Kamiryo et al. 2001, Liscák et al. 2002, Jirák et al. 2007, Liang et al. 2008, Charest et al. 2009, Hirano et al. 2009, Massager et al. 2009a, 2009b, Marcelin et al. 2010) or with a linear accelerator (LINAC)-based approach (Ernst-Stecken et al. 2007). Arc therapy with the application of cylindrical collimators allows the irradiation of subregions of the skull of one subject animal (Reinacher et al. 1999, Münter et al. 2001) and the addition of image guidance of cone beam CT results in increased accuracy (Tan et al. 2011). We performed a dose-de-escalation from 120–40 Gy in 10 Gy steps. The morphological and functional changes detected were clearly related to the radiation dose. The 2-weekly assessment of open-field tests did not reveal any behavioural alteration, apart from the rats irradiated at 120–110 Gy, which displayed an obvious deterioration. Only the changes in rearing activity indicated the effects of the focal brain injury; these were first observed 40–55 days post-irradiation at the 90 Gy dose level. In the course of its explorations, the rat gains information about its environment, and it continues this activity until it can develop an integrated concept of the situation. One of the most important roles of the hippocampus is to achieve this integration, and in normal rats this proceeds well. Rats with an impaired dorsal hippocampus require more extensive exploration to attain the same result. The changes in spontaneous locomotor activity mostly depend on the nature and magnitude of the lesions (Leggio et al. 2006, Alstott et al. 2009). In our experiments, the slight changes in locomotor activity can be explained by the short time frame of the open-field tests. These revealed that the effects of relevant damage in the motor cortex start to become observable 8 weeks after irradiation, which corresponds well to the development of an irreversible human focal brain injury (Godsil et al. 2005, Huang et al. 2009, Caceres et al. 2010). Nevertheless, we do not consider the open-field activity to be a highly sensitive tool for the detection of changes due to radiation damage. A subsequent detailed analysis of our data demonstrated that the locomotor deterioration could be measured at high dose levels and at later time points than 2 months after the treatment. In planned studies, therefore, we intended to perform open-field tests at 2-week intervals up to 6 months. The MWM test is widely used for the detection of neurofunctional impairments (Justino et al. 1997, Yoneoka et al. 1999, Akiyama et al. 2001, Liscák et al. 2002, Vorhees & Williams 2006, Jirák et al. 2007, Shi et al. 2011). In our model, the memory decline first appeared between 30 and 120 days after the irradiation, clearly depending on the dose delivered. The behavioural impairment correlated closely with the morphological changes detected by MRI and histology. Numerous publications have described different methods and reported on the value of MRI examinations for the detection of changes (even at a molecular level) due to ionizing radiation in a small-animal brain.

The radiation-induced morphological changes demonstrated by repeated MRI scans correlated well with the dose, the duration and location of the lesion (Karger et al. 1997, Ishikawa et al. 1999, Brisman et al. 2003). Single doses of 150 Gy or 100 Gy produced necrosis in the hippocampus within 1–3 months (Liscák et al. 2002) and 75 Gy caused a focal brain lesion within 3–6 months (Liscák et al. 2002, Jirák et al. 2007). At doses higher than 60 Gy, necrotic changes started to appear within 6 months (Liscák et al. 2002, Brisman et al. 2003), and 20 months after lower doses, such as 25–50 Gy, delivered to the right frontal lobe of rats, MRI changes were demonstrated in relaxation times T1 and T2 (Karger et al. 1997, Ishikawa et al. 1999). We set out to perform simultaneous MRI examinations on 6 rats with the available 1.5 T device and a human brain coil in order to detect and follow up the necrotic changes *in vivo*, and to optimize the time point of histopathologic examinations. Our method proved simple and effective, with a relatively high throughput, and the results exhibited a clear correspondence with the histopathological findings. The H&E slides showed that the irradiation was localized to a defined small brain volume and the effects in the animals were well reproducible: the damage appeared only in the irradiated region. We did not observe histopathological aberrations in the contralateral hemisphere or in the control animals. This proves the efficacy of the irradiation method. The induced changes depended strongly on the radiation dose.

Significant correlations were detected between the radiation dose and the degree of necrosis, the presence of foamy macrophages, the vascularization and the calcification. Previous studies have indicated that histopathological structural changes involving a decrease in the cell number and demyelination can be expected in the dose range 50–100 Gy (Kamiryo et al. 2001, Liscák et al. 2002, Ernst-Stecken et al. 2007). With such doses, our histopathological analysis revealed measurable 6 x 8 mm necrotic lesions with cysta ex emollition, haemorrhage and a reactive cellular response. In confirmation of earlier data (Münter et al. 1999, Liscák et al. 2002, Jirák et al. 2007, Kumar et al. 2012), the severity of the radiation damage was strictly dose-dependent.

Testing radiation injury and potential radiation modifiers

The various new radiation techniques encourage escalation of the dose in the treatment of primary and secondary brain tumours, though this is accompanied by an increase in the probability of complications in the healthy regions of the brain, while the concurrent chemotherapy applied in cases of glioblastoma results in a rise in the number of treatment-related injuries (Brandsma et al. 2008; Chamberlain et al. 2007; de Wit et al. 2004). On the other hand, the rising number of cases of human stereotactic radiosurgery (SRS) in which a single dose of 18–26 Gy is applied verify the clinical relevance of investigations on single dose delivery. In clinical series of SRS, the

development of brain necrosis has been reported with probabilities of 25–40%. If the level of cognitive reduction could be lessened, the QOL of the survivors would improve and the social and economic strain would be reduced. There is therefore a great need for a potent radioprotector which could decrease the extent of damage to the healthy brain.

The hippocampus is the major brain area that plays a crucial role in the processes of learning and memory (Izquierdo & Medina 1997; Gil-Mohapel et al. 2013), and numerous data clearly confirm that irradiation causes a deterioration of these functions (Rola et al. 2004; Raber 2010; Yazlovitskaya et al. 2006). In the hippocampus, the dentate gyrus is the region most susceptible to radiation (Monje 2008), because this is the site of neurogenesis (Monje & Palmer 2003; Zhao et al. 2008). Our earlier study of the dose–response relationship indicated that the chosen model is relevant for studying various aspects of healthy brain protection (Hideghéty et al. 2013).

In our present investigation, this method revealed a promising ameliorative effect of GPC, which can be explained by its role in preserving the cell membranes and cognitive functions in the CNS. Choline and choline-containing phospholipids such as GPC display mainly a cholinergic profile, interfering with phospholipids biosynthesis, brain metabolism and neurotransmitter systems, and are responsible for maintaining the cell membrane integrity and are also precursors of the neurotransmitter acetylcholine, which is involved in a number of brain processes, including learning and memory (Tayebati et al. 2013). GPC has previously been studied as a centrally acting parasympathomimetic drug in acute cerebrovascular diseases and dementia disorders (Barbagallo Sangiorgi et al. 1994; Parnetti et al. 2001). After oral administration, GPC can cross the BBB and reach the CNS, where it can exert beneficial effects in the treatment of the sequelae of cognitive disorders and cerebrovascular accidents. It can incorporate into the phospholipid fraction of the neuronal plasma membrane and can also increase the levels of production and release of acetylcholine in the brain (Amenta & Tayebati 2008; Tayebati et al. 2011; Tayebati et al. 2013). A trial of the clinical efficacy and tolerability of GPC on 2044 patients after stroke or transient ischaemic attacks confirmed the therapeutic efficacy of GPC in the cognitive recovery, the presumed mechanism involving the provision of a high level of choline for the nervous cells, which protects their cell membranes (Barbagallo Sangiorgi et al. 1994).

Our study clearly illustrates the protective effects of GPC at both functional and morphological levels. The cognitive dysfunction resulting from irradiation can be examined by different methods. The MWM has been found to be a highly sensitive tool for the detection of a neurofunctional impairment (Akiyama et al. 2001; Jirák et al. 2007; Justino et al. 1997; Liscák et al. 2002; Shi et al. 2011; Vorhees & Williams 2006; Yoneoka et al. 1999). The MWM task clearly demonstrated the effects of GPC on the working memory and long-lasting reference memory of rats after irradiation at

a 40 Gy dose level, the differences in learning ability between the RT and CO groups becoming more pronounced as time passed.

An earlier analysis of the histological changes led to the finding that brain irradiation modified the spine density and also the proportions of the morphological subtypes in the dendrites of the dentate gyrus granule cells and the basal dendrites of the CA1 pyramidal neurones, in a time-dependent manner (Chakraborti et al. 2012). Pathological disturbances such as vascular damage and demyelination are late consequences of irradiation that are likewise revealed by histological examination (Brown et al. 2005). The primary targets of radiation damage include the oligodendrocytes and the white matter, which suffer necrosis (Shen et al. 2012; Valk & Dillon 1991). In our study, the levels of such histopathological deterioration, scored semiquantitatively, were ameliorated significantly by GPC treatment. The changes in cognitive ability correlated closely with the histopathological findings indicative of the radio-neuroprotecive action of GPC.

VI. CONCLUSIONS AND FINDINGS

The investigation of the potential neuroprotectors resulted in the exclusion of the MRP approach from further research and warranted the performance of further preclinical examinations on the kynurenine pathway and with phosphatidylcholine derivatives.

We have carefully examined numerous MRP inhibitors/stimulators, which did not significantly influence the striatal levels of DA and its metabolites. Although, NGN mildly mitigated the DA level reduction, this did not reach the level of significance.

We experienced the opposite effect of AP, which considerably intensified the MPTP-induced lethality. The possible explanation of these findings could involve stimulation of the MRP1- and MRP2-mediated transport of the protective GSH conjugates which act against toxic agents, or possibly the enhancement of the oxidative stress caused by the MRP4-mediated efflux of brain uric acid, which has marked antioxidant activity.

Our next approach to achieve a protective effect in the CNS was the use of different analogues that play key roles in the kynurenine pathway. The analysis of several KYNA analogues provided a growing body of data concerning the effects of these compounds in mouse models. Our experiments proved the good tolerability of these agents, without notable toxic effects. These agents could therefore be examined in our newly-developed small-animal model.

Within the neurofunctional examinations on drug tolerability, particularly the value of an open-field task could be demonstrated in investigations of locomotor activity and explorative behaviour.

The partial rat brain irradiation technique that we have developed with the human stereotactic BrainLab system, provides a high-precision, single dose delivery at the same time to 2 animals. It causes a pronounced brain injury in a predetermined volume.

We have also developed a well-reproducible small-animal radiation model for 6 rats that results in dose-dependent focal brain damage limited to one hemisphere.

In addition, a complex and reliable system of examinations on functional and morphological alterations was developed with which the radiation-induced late changes in the CNS could be followed in a small-animal model appropriate for investigations on radiation modifiers.

We have derived a dose–effect curve of radiosensitivity via the MWM test, exhibiting the effects of differences between 10 Gy dose levels. The MWM test proved to be the most sensitive method among the neurofunctional examinations.

Our data have provided experimental evidence of the changes in cognitive function and histological deterioration after the irradiation of one hemispherical hippocampus and the potential for GPC

treatment to exert a favourable influence on such events. This study warrants further research on the protective or mitigating effects of GPC on radiation injuries.

VII. ACKNOWLEDGEMENTS

I would like to thank Professor László Vécsei, Member of the Hungarian Academy of Sciences, Head of the Department of Neurology, University of Szeged, for the opportunity to work in his laboratory and for his valuable scientific advice. I would also like to express my gratitude to my supervisor, Péter Klivényi M.D., Ph.D., for his scientific guidance. Many thanks are due to Katalin Hideghéty M.D., Ph.D., Associate Professor at the Department of Oncotherapy, University of Szeged, for her scientific advice, her continuous support of my research activities and her sustained trust in me.

I wish to thank all those co-workers with whom I performed the experiments, and especially Dénes Zádori M.D., Ph.D. and Tünde Tőkés B.Sc., Ph.D.

I would like to acknowledge the technical assistance of Valéria Széll Vékonyné, Andrea Tóth, Imola Mán and Emília Rita Szabó.

I wish to express my special gratitude to my family and friends for their endless support during my work.

VIII. REFERENCES

1. Agid Y. Parkinson's disease: pathophysiology. Lancet 1991; 337: 1321–1324.
2. Akiyama K, Tanaka R, Sato M, Takeda N. Cognitive dysfunction and histological findings in adult rats one year after whole brain irradiation. Neurol Med Chir (Tokyo) 2001; 41: 590–598.
3. Alstott J, Breakspear M, Hagmann P, Cammoun L, Sporns O. Modeling the impact of lesions in the human brain. PLoS Comput Biol 2009; 5: e1000408.
4. Amenta F, Liu A, Zeng YC, Zaccheo D. Muscarinic cholinergic receptors in the hippocampus of aged rats: influence of choline alphoscerate treatment. Mech Ageing Dev 1994; 76: 49–64.
5. Amenta F, Tayebati SK. Pathways of acetylcholine synthesis, transport and release as targets for treatment of adult-onset cognitive dysfunction. Curr Med Chem 2008; 15: 488–498.
6. Attanasi F, Belcari N, Camarda M, Del Guerra A, Moehrs S, Rosso V, Vecchio S, Lanconelli N, Cirrone GA, Di Rosa F, Russo G. Experimental validation of the filtering approach for dose monitoring in proton therapy at low energy. Phys Med 2008; 24: 102–106.
7. Ayrton A, Morgan P. Role of transport proteins in drug absorption, distribution and excretion. Xenobiotica 2001; 31: 469–497.
8. Bakos E, Evers R, Sinko E, Varadi A, Borst P, Sarkadi B. Interactions of the human multidrug resistance proteins MRP1 and MRP2 with organic anions. Mol Pharmacol 2000; 57: 760–768.
9. Barbagallo Sangiorgi G, Barbagallo M, Giordano M, Meli M, Panzarasa R. Alpha-glycerophosphocholine in the mental recovery of cerebral ischemic attacks. An Italian multicenter clinical trial. Ann N Y Acad Sci 1994; 717: 253–269.
10. Bari F, Nagy K, Guidetti P, Schwarcz R, Busija DW, Domoki F. Kynurenic acid attenuates NMDA-induced pial arteriolar dilation in newborn pigs. Brain Res 2006; 1069: 39–46.
11. Beaulieu E, Demeule M, Ghitescu L, Beliveau R. P-glycoprotein is strongly expressed in the luminal membranes of the endothelium of blood vessels in the brain. Biochem J 1997; 326: 539–544.
12. Beşe NS, Uzel O, Turkan S, Okkan S. Continuous hyperfractionated accelerated radiotherapy in the treatment of high-grade astrocytomas. Radiother Oncol 1998; 47: 197–200.
13. Borst P, Elferink RO. Mammalian ABC transporters in health and disease. Annu Rev Biochem 2002; 71: 537–592.

14. Brandsma D, Stalpers L, Taal W, Sminia P, van den Bent MJ. Clinical features, mechanisms and management of pseudoprogression in malignant gliomas. Lancet Oncol 2008; 9: 453–461.
15. Bredesen DE, Rao RV, Mehlen P. Cell death in the nervous system. Nature 2006; 443: 796–802.
16. Brisman JL, Cole AJ, Cosgrove GR, Thornton AF, Rabinov J, Bussiere M, Bradley-Moore M, Hedley-Whyte T, Chapman PH. Radiosurgery of the rat hippocampus: Magnetic resonance imaging, neurophysiological, histological, and behavioral studies. Neurosurg 2003; 53: 951–961.
17. Brown WR, Thore CR, Moody DM, Robbins ME, Wheeler KT. Vascular damage after fractionated whole-brain irradiation in rats. Radiat Res 2005; 164: 662–668.
18. Brownawell AM, Carmines EL, Montesano F. Safety assessment of AGPC as a food ingredient. Food Chem Toxicol 2011; 49: 1303–1315.
19. Caceres LG, Aon Bertolino L, Saraceno GE, Zorrilla Zubilete MA, Uran SL, Capani F, Guelman LR. Hippocampal-related memory deficits and histological damage induced by neonatal ionizing radiation exposure. Role of oxidative status. Brain Res 2010; 1312: 67–78.
20. Chakraborti A, Allen A, Allen B, Rosi S, Fike JR. Cranial irradiation alters dendritic spine density and morphology in the hippocampus. PLoS One 2012; 7: e40844.
21. Chamberlain MC, Glantz MJ, Chalmers L, Van Horn A, Sloan AE. Early necrosis following concurrent Temodar and radiotherapy in patients with glioblastoma. J Neurooncol 2007; 82: 81–83.
22. Charest G, Mathieu D, Lepage M, Fortin D, Paquette B, Sanche L. Polymer gel in rat skull to assess the accuracy of a new rat stereotactic Acta Neurochir (Wien) 2009; 151: 677–683.
23. Choudhuri S, Cherrington NJ, Li N, Klaassen CD. Constitutive expression of various xenobiotic and endobiotic transporter mRNAs in the choroid plexus of rats. Drug Metab Dispos 2003; 31: 1337–1345.
24. Cisternino S, Rousselle C, Lorico A, Rappa G, Scherrmann JM. Apparent lack of Mrp1-mediated efflux at the luminal side of mouse blood-brain barrier endothelial cells. Pharm Res 2003; 20: 904–909.
25. Dallas S, Miller DS, Bendayan R. Multidrug resistance-associated proteins: expression and function in the central nervous system. Pharmacol Rev 2006; 58: 140–161.
26. Dauer W, Przedborski S. Parkinson’s disease: mechanisms and models. Neuron 2003; 39: 889–909.

27. De Jesus Moreno Moreno M. Cognitive improvement in mild to moderate Alzheimer's dementia after treatment with the acetylcholine precursor choline alfoscerate: a multicenter, double-blind, randomized, placebo-controlled trial. Clin Ther 2003; 25: 178–193.
28. Desole MS, Esposito G, Fresu L, Migheli R, Sircana S, Delogu R, Miele M, Miele E. Further investigation of allopurinol effects on MPTP-induced oxidative stress in the striatum and brain stem of the rat. Pharmacol Biochem Behav 1996; 54: 377–383.
29. de Wit MC, de Bruin HG, Eijkenboom W, Sillevis PA, van den Bent MJ. Immediate post-radiotherapy changes in malignant glioma can mimic tumor progression. Neurology 2004; 63: 535–537.
30. Dombrowski SM, Desai SY, Marroni M, Cucullo L, Goodrich K, Bingaman W, Mayberg MR, Bengez L, Janigro D. Overexpression of multiple drug resistance genes in endothelial cells from patients with refractory epilepsy. Epilepsia 2001; 42: 1501–1506.
31. Drozdzik M, Bialecka M, Mysliwiec K, Honczarenko K, Stankiewicz J, Sych Z. Polymorphism in the P-glycoprotein drug transporter MDR1 gene: a possible link between environmental and genetic factors in Parkinson's disease. Pharmacogenetics 2003; 13: 259–263.
32. El-Sheikh AA, van den Heuvel JJ, Koenderink JB, Russel FG. Effect of hypouricaemic and hyperuricaemic drugs on the renal urate efflux transporter, multidrug resistance protein 4. Br J Pharmacol 2008; 155: 1066–1075.
33. Ernst-Stecken A, Jeske I, Hess A, Rödel F, Ganslandt O, Grabenbauer G, Sauer R, Brune K, Blümcke I. Hypofractionated stereotactic radiotherapy to the rat hippocampus. Determination of dose response and tolerance. Strahlenther Onkol 2007; 183: 440–446.
34. Evers R, de Haas M, Sparidans R, Beijnen J, Wielinga PR, Lankelma J, Borst P. Vinblastine and sulfinpyrazone export by the multidrug resistance protein MRP2 is associated with glutathione export. Br J Cancer 2000; 83: 375–383.
35. Flood PM, Qian L, Peterson LJ, Zhang F, Shi JS, Gao HM, Hong JS. Transcriptional factor NF-κB as a target for therapy in Parkinson’s disease. Parkinsons Dis 2011; 2011:216298.
36. Floyd NS, Woo SY, Teh BS, Prado C, Mai WY, Trask T, Gildenberg PL, Holoye P, Augspurger ME, Carpenter LS, Lu HH, Chiu JK, Grant WH 3rd, Butler EB. Hypofractionated intensity-modulated radiotherapy for primary glioblastoma multiforme. Int J Radiat Oncol Biol Phys 2004; 58: 721–726.
37. Gallazzini M, Burg MB. What's new about osmotic regulation of glycerophosphocholine. Physiology 2009; 24: 245–249.

38. Gibrat C, Saint-Pierre M, Bousquet M, Lévesque D, Rouillard C, Cicchetti F. Differences between subacute and chronic MPTP mice models: investigation of dopaminergic neuronal degeneration and alpha-synuclein inclusions. J Neurochem 2009; 109: 1469–1482.
39. Gigler G, Szénási G, Simó A, Lévay G, Hársing LG Jr, Sas K, Vécsei L, Toldi J. Neuroprotective effect of L-kynurenine sulfate administered before focal cerebral ischemia in mice and global cerebral ischemia in gerbils. Eur J Pharmacol 2007; 564: 116–122.
40. Gil-Mohapel J, Brocardo PS, Choquette W, Gothard R, Simpson JM, Christie BR. Hippocampal neurogenesis levels predict WATERMAZE search strategies in the aging brain. PLoS One 2013; 8: e75125.
41. Godsil BP, Stefanacci L, Fanselow MS. Bright light suppresses hyperactivity induced by excitotoxic dorsal hippocampus lesions in the rat. Behav Neurosci 2005; 119: 1339–1352.
42. Golden PL, Pardridge WM. P-Glycoprotein on astrocyte foot processes of unfixed isolated human brain capillaries. Brain Res 1999; 819: 143–146.
43. Gollapudi S, Kim CH, Tran BN, Sangha S, Gupta S. Probenecid reverses multidrug resistance in multidrug resistance-associated protein-overexpressing HL60/AR and H69/AR cells but not in P-glycoprotein-overexpressing HL60/Tax and P388/ADR cells. Cancer Chemother Pharmacol 1997; 40: 150–158.
44. Greene-Schloesser D, Moore E, Robbins ME. Molecular pathways: radiation-induced cognitive impairment. Clin Cancer Res 2013; 19: 2294–2300.
45. Hallman H, Olson L, Jonsson G. Neurotoxicity of the meperidine analogue N-methyl-4-phenyl-1,2,3,6-tetrahydropyridine on brain catecholamine neurons in the mouse. Eur J Pharmacol 1984; 97:133–136.
46. Hideghéty K, Plangár I, Mán I, Fekete G, Nagy Z, Volford G, Tőkés T, Szabó ER, Szabó Z, Brinyiczki K, Mózes P, Németh I. Development of a small-animal focal brain irradiation model to study radiation injury and radiation-injury modifiers. Int J Radiat Biol 2013; 89: 645–655.
47. Hirano M, Shibato J, Rakwal R, Kouyama N, Katayama Y, Hayashi M, Masuo Y. Transcriptomic analysis of rat brain tissue following gamma knife surgery: Early and distinct bilateral effects in the unirradiated striatum. Mol Cells 2009; 27: 263–268.
48. Hirsch E, Graybiel AM, Agid YA. Melanized dopaminergic neurons are differentially susceptible to degeneration in Parkinson's disease. Nature 1988; 334: 345–348.

49. Huang Y, Brandon MP, Griffin AL, Hasselmo ME, Eden UT. Decoding movement trajectories through a T-maze using point process filters applied to place field data from rat hippocampal region CA1. Neural Comput 2009; 21: 3305–3334.
50. Ishikawa S, Otsuki T, Kaneki M, Jokura H, Yoshimoto T. Dose-related effects of single focal irradiation in the medial temporal lobe structures in rats – magnetic resonance imaging and histological study. Neurol Med Chir (Tokyo) 1999; 39: 1–7.
51. Izquierdo I, Medina JH. Memory formation: The sequence of biochemical events in the hippocampus and its connection to activity in other brain structures. Neurobiol Learn Mem 1997; 68: 285–316.
52. Jirák D, Náměstková K, Herynek V, Liscák R, Vymazal J, Mares V, Syková E, Hájek M. Lesion evolution after gamma knife irradiation observed by magnetic resonance imaging. Int J Radiat Biol 2007; 83: 237–244.
53. Justino L, Welner SA, Tannenbaum GS, Schipper HM. Long-term effects of cysteamine on cognitive and locomotor behaviour in rats: relationship to hippocampal glial pathology and somatostatin levels. Brain Res 1997; 761: 127–134.
54. Kalm M, Karlsson N, Nilsson MK, Blomgren K. Loss of hippocampal neurogenesis, increased novelty-induced activity, decreased home cage activity, and impaired reversal learning one year irradiation of the young mouse brain. Exp Neurol 2013; 247: 402–409.
55. Kamiryo T, Han K, Golfinos J, Nelson PK. A stereotactic device for experimental rat and mouse irradiation using gamma knife model B – technical note. Acta Neurochir (Wien) 2001; 143: 83–87.
56. Karger CP, Hartmann GH, Peschke P, Debus J, Hoffmann U, Brix G, Hahn EW, Lorenz WJ. Dose-response relationship for late functional changes in the rat brain after radiosurgery evaluated by magnetic resonance imaging. Int J Radiat Oncol Biol Phys 1997; 39: 1163–1172.
57. Kessler M, Terramani T, Lynch G, Baudry M. A glycine site associated with N-methyl-D-aspartic acid receptors: characterization and identification of a new class of antagonists. J Neurochem 1989; 52: 1319–1328.
58. Khandelwal PJ, Herman AM, Moussa CE. Inflammation in the early stages of neurodegenerative pathology. J Neuroimmunol 2011; 238: 1–11.
59. Kiuchi Y, Suzuki H, Hirohashi T, Tyson CA, Sugiyama Y. cDNA cloning and inducible expression of human multidrug resistance associated protein 3 (MRP3). FEBS Lett 1998; 433: 149–152.

60. Knyihar-Csillik E, Mihaly A, Krisztin-Peva B, Robotka H, Szatmari I, Fulop F, Toldi J, Csillik B, Vecsei L. The kynurenate analog SZR-72 prevents the nitroglycerol-induced increase of c-fos immunoreactivity in the rat caudal trigeminal nucleus: comparative studies of the effects of SZR-72 and kynurenic acid. Neurosci Res 2008; 61: 429–432.
61. Kreitman RR, Blanchette F. On the horizon: possible neuroprotective role for glatiramer acetate. Mult Scler 2004; 10: S81–89.
62. Krohn M, Lange C, Hofrichter J, Scheffler K, Stenzel J, Steffen J, Schumacher T, Brüning T, Plath AS, Alfen F, Schmidt A, Winter F, Rateitschak K, Wree A,Gsponer J, Walker LC, Pahnke J. Cerebral amyloid-beta proteostasis is regulated by the membrane transport protein ABCC1 in mice. J Clin Invest 2011; 121: 3924–3931.
63. Kumar S, Arbab AS, Jain R, Kim J, deCarvalho AC, Shankar A, Mikkelsen T, Brown SL. Development of a novel animal model to differentiate radiation necrosis from tumor recurrence. J Neurooncol 2012; 108: 411–420.
64. Kureshi SA, Hofman FM, Schneider JH, Chin LS, Apuzzo ML, Hinton DR. Cytokine expression in radiation-induced delayed cerebral injury. Neurosurgery 1994; 35: 822–830.
65. Langston JW, Forno LS, Tetrud J, Reeves AG, Kaplan JA, Karluk D. Evidence of active nerve cell degeneration in the substantia nigra of humans years after 1-methyl-4-phenyl-1,2,3,6-tetrahydropyridine exposure. Ann Neurol 1999; 46: 598–605.
66. Lau YS, Trobough KL, Crampton JM, Wilson JA. Effects of probenecid on striatal dopamine depletion in acute and long-term 1-methyl-4-phenyl-1,2,3,6-tetrahydropyridine (MPTP)-treated mice. Gen Pharmacol 1990; 21: 181–187.
67. Le Couteur DG, Davis MW, Webb M, Board PG. P-glycoprotein, multidrug-resistance-associated protein and Parkinson's disease. Eur Neurol 2001; 45: 289–290.
68. Lee G, Bendayan R. Functional expression and localization of P-glycoprotein in the central nervous system: relevance to the pathogenesis and treatment of neurological disorders. Pharm Res 2004; 21: 1313–1330.
69. Lee H, Pienaar IS. Disruption of the blood-brain barrier in parkinson’s disease: curse or route to a cure? Front Biosci (Landmark Ed) 2014; 19: 272–280.
70. Lee WH, Warrington JP, Sonntag WE, Lee YW. Irradiation alters MMP-2/TIMP-2 system and collagen type IV degradation in brain. Int J Radiat Oncol Biol Phys 2012; 82: 1559–1566.
71. Leggas M, Adachi M, Scheffer GL, Sun D, Wielinga P, Du G, Mercer KE, Zhuang Y, Panetta JC, Johnston B, Scheper RJ, Stewart CF, Schuetz JD. Mrp4 confers resistance to topotecan and protects the brain from chemotherapy. Mol Cell Biol 2004; 24: 7612–7621.

72. Leggio MG, Federico F, Neri P, Graziano A, Mandolesi L, Petrosini L. NMDA receptor activity in learning spatial procedural strategies I. The influence of hippocampal lesions. Brain Res Bull 2006; 70: 347–355.
73. Leslie EM, Deeley RG, Cole SP. Bioflavonoid stimulation of glutathione transport by the 190-kDa multidrug resistance protein 1 (MRP1). Drug Metab Dispos 2003; 31: 11–15.
74. Liang CD, Li WL, Liu N, Yin Y, Hao J, Zhao WQ. Effects of gamma knife irradiation on the expression of NMDA receptor subunits in rat forebrain. Neurosci Lett 2008; 439: 250–255.
75. Liscák R, Vladyka V, Novotný J Jr, Brozek G, Naměstkova K, Mares V, Herynek V, Jirák D, Hájek M, Syková E. Leksell gamma knife lesioning of the rat hippocampus: the relationship between radiation dose and functional and structural damage. J Neurosurg 2002; 97: 666–673.
76. Lin CY, Hsu YH, Lin MH, Yang TH, Chen HM, Chen YC, Hsiao HY, Chen CC, Chern Y, Chang C. Neurovascular abnormalities in humans and mice with Huntington's disease. Exp Neurol 2013; 250: 20–30.
77. Lunsford LD, Altschuler EM, Flickinger JC, Wu A, Martinez AJ. In vivo biological effects of stereotactic radiosurgery: A primate model. Neurosurgery 1990; 27: 373– 382.
78. Marcelin B, Kjäll P, Johansson J, Lundin A, Nordström H, Eriksson M, Bernard C, Régis J. Using Monte-Carlo-simulated radiation transport to calculate dose distribution in rats before irradiation with Leksell Gamma Knife 4C: Technical note. Stereotact Funct Neurosurg 2010; 88: 208–215.
79. Markey SP, Johannessen JN, Chiueh CC, Bums RS, Herkenham MA. Intraneuronal generation of a pyridinium metabolite may cause drug-induced parkinsonism. Nature 1984; 311: 464–467.
80. Marosi M, Nagy D, Farkas T, Kis Z, Rózsa E, Robotka H, Fülöp F, Vécsei L, Toldi J. A novel kynurenic acid analogue: a comparison with kynurenic acid. An in vitro electrophysiological study. J Neural Transm 2010; 117: 183–188.
81. Massager N, Maris C, Nissim O, Devriendt D, Salmon I, Levivier M. Experimental analysis of radiation dose distribution in radiosurgery: I. Dose hot spot inside target volume. Stereotact Funct Neurosurg 2009a; 87: 82–87.
82. Massager N, Maris C, Nissim O, Devriendt D, Salmon I, Levivier M. Experimental analysis of radiation dose distribution in radiosurgery. II. Dose fall-off outside the target volume. Stereotact Funct Neurosurg 2009b; 87: 137–142.
83. Meredith GE, Totterdell S, Potashkin JA, Surmeier DJ. Modeling PD pathogenesis in mice: advantages of a chronic MPTP protocol. Parkinsonism Relat Disord 2008; 14: S112–115.

84. Miele M, Esposito G, Migheli R, Sircana S, Zangani D, Fresu GL, Desole MS. Effects of allopurinol on 1-methyl-4-phenyl-1,2,3,6-tetrahydropyridine (MPTP)-induced neurochemical changes in the striatum and in the brainstem of the rat. Neurosci Lett 1995; 183: 155–159.
85. Miller DS, Nobmann SN, Gutmann H, Toeroek M, Drewe J, Fricker G. Xenobiotic transport across isolated brain microvessels studied by confocal microscopy. Mol Pharmacol 2000; 58: 1357–1367.
86. Monje M. Cranial radiation therapy and damage to hippocampal neurogenesis. Dev Disabil Res Rev 2008; 14: 238–242.
87. Monje ML, Palmer T. Radiation injury and neurogenesis. Curr Opin Neurol 2003; 16: 129–134.
88. Moore ED, Kooshki M, Metheny-Barlow LJ, Gallagher PE, Robbins ME. Angiotensin-(1-7) prevents radiation-induced inflammation in rat primary astrocytes through regulation of MAP kinase signaling. Free Radic Biol Med 2013; 65:1060–1068.
89. Münter MW, Karger CP, Reith W, Schneider HM, Peschke P, Debus J. Delayed vascular injury after single high-dose irradiation in the rat brain: Histologic immunohistochemical, and angiographic studies. Radiology 1999; 212: 475–482.
90. Münter MW, Karger CP, Schröck H, de Vries A, Schneider HM, Wannenmacher M, Debus J. Late radiation changes after small volume radiosurgery of the rat brain. Measuring local cerebral blood flow and histopathological studies. Strahlenther Onkol 2001; 177: 354–361.
91. Na A, Haghigi N, Drummond KJ. Cerebral radiation necrosis. Asia Pac J Clin Oncol 2014; 10: 11–21.
92. Németh H, Robotka H, Kis Z, Rózsa E, Janáky T, Somlai C, Marosi M, Farkas T, Toldi J, Vécsei L. Kynurenine administered together with probenecid markedly inhibits pentylenetetrazol-induced seizures. An electrophysiological and behavioural study. Neuropharmacology 2004; 47: 916–925.
93. Németh H, Toldi J, Vécsei L. Kynurenines, Parkinson's disease and other neurodegenerative disorders: preclinical and clinical studies. J Neural Transm Suppl 2006; 70: 285–304.
94. Nies AT, Jedlitschky G, Konig J, Herold-Mende C, Steiner HH, Schmitt HP, Keppler D. Expression and immunolocalization of the multidrug resistance proteins, MRP1-MRP6 (ABCC1-ABCC6), in human brain. Neuroscience 2004; 129: 349–360.
95. Nishino J, Suzuki H, Sugiyama D, Kitazawa T, Ito K, Hanano M, Sugiyama Y. Transepithelial transport of organic anions across the choroid plexus: possible involvement

of organic anion transporter and multidrug resistance-associated protein. J Pharmacol Exp Ther 1999; 290: 289–294.

96. Olney JW. Brain lesions, obesity, and other disturbances in mice treated with monosodium glutamate. Science 1969; 164: 719–721.
97. Onishchenko LS, Gaikova ON, Yanishevskii SN. Changes at the focus of experimental ischemic stroke treated with neuroprotective agents. Neurosci Behav Physiol 2008; 38:49–54.
98. Parnetti L, Amenta F, Gallai V. Choline alphoscerate in cognitive decline and in acute cerebrovascular disease: an analysis of published clinical data. Mech Ageing Dev 2001; 122: 2041–2055.
99. Parnetti L, Mignini F, Tomassoni D, Traini E, Amenta F. Cholinergic precursors in the treatment of cognitive impairment of vascular origin: ineffective approaches or need for re-evaluation? J Neurol Sci 2007; 257: 264–269.
100. Pedersen JM, Matsson P, Bergstrom CA, Norinder U, Hoogstraate J, Artursson P. Prediction and identification of drug interactions with the human ATP-binding cassette transporter multidrug-resistance associated protein 2 (MRP2; ABCC2). J Med Chem 2008; 51: 3275–3287.
101. Prasad KN. Rationale for using multiple antioxidants in protecting humans against low doses of ionizing radiation. Br J Radiol 2005; 78:485–492.
102. Raber J. Unitended effects of cranial irradiation on cognitive function. Toxicol Pathol 2010; 38: 198–202.
103. Rao VV, Dahlheimer JL, Bardgett ME, Snyder AZ, Finch RA, Sartorelli AC, Piwnica-Worms D. Choroid plexus epithelial expression of MDR1 P glycoprotein and multidrug resistance-associated protein contribute to the blood-cerebrospinal-fluid drug-permeability barrier. Proc Natl Acad Sci U S A 1999; 96: 3900–3905.
104. Reichmann H, Riederer P. Biochemical analyses of respiratory chain enzymes in different brain regions of patients with Parkinson's disease. BMFT Symposium "Morbus Parkinson und andere Basalganglienerkrankungen". Bad Kissingen. 1989; p. 44 (abstract).
105. Reid G, Wielinga P, Zelcer N, De Haas M, Van Deemter L, Wijnholds J, Balzarini J, Borst P. Characterization of the transport of nucleoside analog drugs by the human multidrug resistance proteins MRP4 and MRP5. Mol Pharmacol 2003; 63: 1094–1103.
106. Reinacher PC, Blum C, Gass P, Karger CP, Debus J. Quantification of microglial late reaction to stereotactic irradiation of the rat brain using computer-aided image analysis. Exp Neurol 1999; 160: 117–123.

107. Renes J, de Vries EE, Hooiveld GJ, Krikken I, Jansen PL, Muller M. Multidrug resistance protein MRP1 protects against the toxicity of the major lipid peroxidation product 4-hydroxynonenal. Biochem J 2000; 350: 555–561.
108. Roberts LM, Black DS, Raman C, Woodford K, Zhou M, Haggerty JE, Yan AT, Cwirla SE, Grindstaff KK. Subcellular localization of transporters along the rat blood-brain barrier and blood-cerebral-spinal fluid barrier by in vivo biotinylation. Neuroscience 2008; 155: 423–438.
109. Roberge D, Petrecca K, El Refae M, Souhami L. Whole-brain radiotherapy and tumor bed radiosurgery following resection of solitary brain metastases. J Neurooncol 2009; 95: 95–99.
110. Rola R, Raber J, Rizk A, Otsuka S, Van den Berg SR, Morhardt DR, Fike JR. Radiation-induced impairment of hippocampal neurogenesis is associated with cognitive deficits in young mice. Exp Neurol 2004; 188: 316–330.
111. Roman DD, Sperduto PW. Neuropsychological effects of cranial radiation: current knowledge and future directions. Int J Radiat Oncol Biol Phys 1995; 31: 983–998.
112. Ross JA, Kasum CM. Dietary flavonoids: bioavailability, metabolic effects, and safety. Annu Rev Nutr 2002; 22: 19–34.
113. Saller R, Melzer J, Reichling J, Brignoli R, Meier R. An updated systematic review of the pharmacology of silymarin. Forsch Komplementmed 2007; 14: 70–80.
114. Savitt JM, Dawson VL, Dawson TM. Diagnosis and treatment of Parkinson disease: molecules to medicine. J Clin Invest 2006; 116: 1744–1754.
115. Schapira AH, Cooper JM, Dexter D, Jenner P, Clark JB, Marsden CD. Mitochondrial complex I deficiency in Parkinson’s disease. Lancet 1989; 1: 1269.
116. Schinkel AH, Smit JJ, van Tellingen O, Beijnen JH, Wagenaar E, van Deemter L, Mol CAAM, van der Valk MA, Robanus-Maandag EC, te Riele HPJ, Berns AJM, Borst P. Disruption of the mouse mdr1a P-glycoprotein gene leads to a deficiency in the blood-brain barrier and to increased sensitivity to drugs. Cell 1994; 77: 491–502.
117. Scribner DM, Witowski NE, Mulier KE, Lusczek ER, Wasiluk KR, Beilman GJ. Liver metabolomic changes identify biochemical pathways in hemorrhagic shock. J Surg Res 2010; 164: 131–139.
118. Shen C, Bao W, Yang B, Xie R, Cao X, Luan SH, Mao Y. Cognitive deficits in patients with brain tumor. Chin Med J 2012; 125: 2610–2617.
119. Shi C, Guo B, Cheng CY, Esquivel C, Enq T, Papanikolaou N. Three dimensional intensity modulated brachytherapy (IMBT): dosimetry algorithm and inverse treatment planning. Med Phys 2010; 37: 3725–3737.

120. Shi L, Linville MC, Iversen E, Molina DP, Yester J, Wheeler KT, Robbins ME, Brunso-Bechtold JK. Maintenance of white matter integrity in a rat model of radiation-induced cognitive impairment. J Neurol Sci 2009; 285: 178–184.
121. Shi L, Olson J, D'Agostino R Jr, Linville C, Nicolle MM, Robbins ME, Wheeler KT, Brunso-Bechtold JK. Aging masks detection of radiation-induced brain injury. Brain Res 2011; 1385: 307–316.
122. Silverman JA. Multidrug-resistance transporters. Pharm Biotechnol 1999; 12: 353–386.
123. Simon S, Desmedt F, Vanderlinden B, Gevaert T, Vanderkerkhove C, Grell AS, Levivier M. Medical physics principles of radiosurgery. Prog Neurol Surg 2007; 20: 43–49.
124. Singhal NK, Srivastava G, Patel DK, Jain SK, Singh MP. Melatonin or silymarin reduces maneb- and paraquat-induced Parkinson's disease phenotype in the mouse. J Pineal Res 2011; 50: 97–109.
125. Soontornmalai A, Vlaming ML, Fritschy JM. Differential, strain-specific cellular and subcellular distribution of multidrug transporters in murine choroid plexus and blood-brain barrier. Neuroscience 2006; 138: 159–169.
126. Spiegelmann R, Friedman WA, Bova FJ, Theele DP, Mickle JP. LINAC radiosurgery: An animal model. J Neurosurg 1993; 78: 638–644.
127. Staal RG, Yang JM, Hait WN, Sonsalla PK. Interactions of 1-methyl-4-phenylpyridinium and other compounds with P-glycoprotein: relevance to toxicity of 1-methyl-4-phenyl-1,2,3,6-tetrahydropyridine. Brain Res 2001; 910: 116–125.
128. Sugiyama D, Kusuhara H, Shitara Y, Abe T, Meier PJ, Sekine T, Endou H, Suzuki H, Sugiyama Y. Characterization of the efflux transport of 17beta-estradiol-D-17beta-glucuronide from the brain across the blood-brain barrier. J Pharmacol Exp Ther 2001; 298: 316–322.
129. Tanner CM and Goldman SM. Epidemiology of Parkinson’s disease. Neurol Clin 1996; 14: 317–335.
130. Sun CC, Luo FF, Wei L, Lei M, Li GF, Liu ZL, LE WD, Xu PY. Association of serum uric acid levels with the progression of Parkinson's disease in Chinese patients. Chin Med J (Engl) 2012; 125: 583–587.
131. Tan YF, Rosenzweig S, Jaffray D, Wojtowicz JM. Depletion of new neurons by image guided irradiation. Front Neurosci 2011; 5: 59.
132. Tayebati SK, Tomassoni D, Di Stefano A, Sozio P, Cerasa LS, Amenta F. Effect of choline-containing phospholipids on brain cholinergic transporters in the rat. J Neurol Sci 2011; 302: 49–57.

133. Tayebati SK, Tomassoni D, Nwankwo IE, Di Stefano A, Sozio P, Cerasa LS, Amenta F. Modulation of monoaminergic transporters by choline-containing phospholipids in rat brain. CNS Neurol Disord Drug Targets 2013; 12: 94–103.

134. Tiller-Borcich JK, Fike JR, Phillips TL, Davis RL. Pathology of delayed radiation brain damage: An experimental canine model. Radiation Research 1987; 110: 161– 172.

135. Tsien C, Moughan J, Michalski JM, Gilbert MR, Purdy J, Simpson J, Kresel JJ, Curran WJ, Diaz A, Mehta MP, Radiation Therapy Oncology Group Trial 98-03. Phase I three-dimensional conformal radiation dose escalation study in newly diagnosed glioblastoma: Radiation Therapy Oncology Group Trial 98-03. Int J Radiat Oncol Biol Phys 2009; 73: 699–708.

136. Valk PE, Dillon WP. Radiation injury of the brain. AJNR Am J Neuroradiol 1991; 12: 45–62.

137. Van Aubel RA, Smeets PH, van den Heuvel JJ, Russel FG. Human organic anion transporter MRP4 (ABCC4) is an efflux pump for the purine end metabolite urate with multiple allosteric substrate binding sites. Am J Physiol Renal Physiol 2005; 288: F327–333.

138. van Veen HW, Konings WN. The ABC family of multidrug transporters in microorganisms. Biochim Biophys Acta 1998; 1365: 31–36.

139. Vámos E, Párdutz A, Varga H, Bohár Z, Tajti J, Fülöp F, Toldi J, Vécsei L. L-kynurenine combined with probenecid and the novel synthetic kynurenic acid derivative attenuate nitroglycerin-induced nNOS in the rat caudal trigeminal nucleus. Neuropharmacology 2009; 57: 425–429.

140. Vinchon-Petit S, Jarnet D, Jadaud E, Feuvret L, Garcion E, Menei P. External irradiation models for intracranial 9L glioma studies. J Exp Clin Cancer Res 2010; 29: 142.

141. Volinsky R, Kinnunen PK. Oxidized phosphatidylcholines in membrane-level cellular signaling: from biophysics to physiology and molecular pathology. FEBS J 2013; 280: 2806–2816.

142. Vorhees CV, Williams MT. Morris water maze: procedures for assessing spatial and related forms of learning and memory. Nat Protoc 2006; 1: 848–858.

143. Wijnholds J, deLange EC, Scheffer GL, van den Berg DJ, Mol CA, van der Valk M, Schinkel AH, Scheper RJ, Breimer DD, Borst P. Multidrug resistance protein 1 protects the choroid plexus epithelium and contributes to the blood-cerebrospinal fluid barrier. J Clin Invest 2000; 105: 279–285.

144. Wu CP, Calcagno AM, Hladky SB, Ambudkar SV, Barrand MA. Modulatory effects of plant phenols on human multidrug-resistance proteins 1, 4 and 5 (ABCC1, 4 and 5). FEBS J 2005; 272: 4725–4740.
145. Yamaguchi N, Yamashima T, Yamashita J. A histological and flow cytometric study of dog brain endothelial cell injuries in delayed radiation necrosis. J Neurosurg 1991; 74: 625–632.
146. Yang T, Wu SL, Liang JC, Rao ZR, Ju G. Time-dependent astroglial changes after gamma knife radiosurgery in the rat forebrain. Neurosurgery 2000; 47: 407–415.
147. Yazlovitskaya EM, Edwards E, Thotala D, Fu A, Osusky KL, Whetsell WO Jr, Boone B, Shinohara ET, Hallahan DE. Lithium treatment prevents neurocognitive deficit resulting from cranial irradiation. Cancer Res 2006; 66: 11179–11186.
148. Yoneoka Y, Satoh M, Akiyama K, Sano K, Fujii Y, Tanaka R. An experimental study of radiation-induced cognitive dysfunction in an adult rat model. Br J Radiol 1999; 72: 1196–1201.
149. Zbarsky V, Datla KP, Parkar S, Rai DK, Aruoma OI, Dexter DT. Neuroprotective properties of the natural phenolic antioxidants curcumin and naringenin but not quercetin and fisetin in a 6-OHDA model of Parkinson's disease. Free Radic Res 2005; 39: 1119–1125.
150. Zhao C, Deng W, Gage FH. Mechanisms and functional implications of adult neurogenesis. Cell 2008; 132: 645–660.
151. Zhou SF, Wang LL, Di YM, Xue CC, Duan W, Li CG, Li Y. Substrates and inhibitors of human multidrug resistance associated proteins and the implications in drug development. Curr Med Chem 2008; 15: 1981–2039.

ANNEX 1.

Imola Plangár, Dénes Zádori, Levente Szalárdy, László Vécsei, Péter Klivényi: Assessment of the role of multidrug resistance-associated proteins in MPTP neurotoxicity in mice. Ideggyógyászati Szemle 2013; 66: 407–414.

ANNEX 2.

Károly Nagy, **Imola Plangár,** Bernadett Tuka, Levente Gellért, Dániel Varga, Ildikó Demeter, Tamás Farkas, Zsolt Kis, Máté Marosi, Dénes Zádori, Péter Klivényi, Ferenc Fülöp, István Szatmári, László Vécsei, József Toldi: Synthesis and biological effects of some kynurenic acid analogs. Bioorganic & Medicinal Chemistry 2011; 19:7590–7596.

ANNEX 3.

Judit Kalincsák, Róbert Farkas, Péter Kovács, Mihály Aradi, Szabolcs Bellyei, Roland Weiczner, Zsolt Sebestyén, Imola Plangár, Katalin Hideghéty: Single dose irradiation of defined region of rat brain with stereotactic BrainLab system. Ideggyógyászati Szemle (ahead of print)

ANNEX 4.

Katalin Hideghéty, **Imola Plangár,** Imola Mán, Gábor Fekete, Zoltán Nagy, Gábor Volford, Tünde Tőkés, Emília Rita Szabó, Zoltán Szabó, Kitti Brinyiczki, Petra Mózes, István Balázs Németh: Development of a small-animal focal brain irradiation model to study radiation injury and radiation-injury modifiers. International Journal of Radiation Biology 2013; 89:645–655.

ANNEX 5.

Imola Plangár, Emília Rita Szabó, Tünde Tőkés, Imola Mán, Kitti Brinyiczki, Gábor Fekete, István Balázs Németh, Miklós Ghyczy, Mihály Boros, Katalin Hideghéty: Radio-neuroprotective effect of L-alpha-glycerylphosphorylcholine (GPC) in an experimental rat model. Journal of Neurooncology (under review)

EGYETEMI DOKTORI ÉRTEKEZÉS – MAGYAR NYELVŰ ÖSSZEFOGLALÓ

Kutatásaink középpontjában a neurodegeneratív folyamatok, a sugárzás-indukálta agyi károsodások, illetve ezek esetleges kivédésének kisállat modellekben történő vizsgálata áll. A neurodegeneratív betegségeknek és a sugárzás-indukálta agyi károsodásoknak számos közös jellemzője van. A sugárzás hatására kialakuló szövettani és sejtszintű elváltozások jelentős mértékben hasonlítanak a neurodegeneratív folyamatok eredményeként manifesztálódó neurodestruktív elváltozásokhoz, sejtpusztuláshoz. Mindkettőre igaz tehát a progresszív neuronpusztulás, a motoros és kognitív funkcióbeli hanyatlás. Hasonlóság van, a következményként megjelenő, különböző mértékű gyulladásos folyamatok előfordulásában is. A neuronpusztulás kezdetétől az első, egyértelmű klinikai tünetek megjelenéséig általában évek, évtizedek telnek el, amely idő alatt a sejtek túlnyomú többsége érintetté válik.

A Parkinson-kór (PK) egy progresszív jellegű neurodegeneratív kórkép, amelyben a substantia nigra pars compacta (SNpc) dopaminerg idegsejtjeinek pusztulása figyelhető meg. A mitokondriális komplex I szelektív gátlásával lehetségessé válik a PK állatkísérletes előidézése. Erre alkalmas vegyület az 1-methyl-4-phenyl-1,2,3,6-tetrahydropyridine (MPTP), amit a gliális monoaminooxidáz 1-methyl-4-phenylpyridiniummá (MPP^+) alakít, amely a dopamin transzporteren keresztül képes a SNpc dopaminerg sejtjeibe jutni, és itt a légzési lánc I-es komplexének működését gátolni. A légzési lánc gátlásának eredménye megnövekedett szabadgyök képződés, illetve ATP depléció, ami rövid időn belül sejtpusztuláshoz vezet.

A központi idegrendszeri tumorok incidenciája folyamatosan növekszik, a sugárkezelés a standard komplex terápia elengedhetetlen része mind primer, mind szekunder, azaz metasztatikus agytumorok esetén. Az agy radiogen nekrózisa a malignus tumorok miatt végzett sugárkezelés súlyos, jelenleg nem kezelhető, irreverzibilis szövődménye, az agresszív malignus központi idegrendszeri tumorok hatékony sugárkezelésének akadálya. A tumort nagy valószínűséggel elpusztító dózis az agy, ill. a gerincvelő viszonylagosan alacsony sugár-toleranciája miatt nem adható le. Amennyiben hatékony neuroprotektív gyógyszer állna rendelkezésünkre, a terápiás index (tumor ellenes hatás/mellékhatás arány) lényegesen javítható lenne.

A központi idegrendszerben a triptofán oxidatív metabolizmusa során keletkező metabolitok megváltoztatják az agyszövet excitabilitását. Azok a szerek, amelyek gátolják a glutamátreceptor-agonista metabolitok (kvinolinsav), valamint a szabadgyök-generált hatásokat, potenciálisan neuroprotektív hatásúak lehetnek. A kinurénsav (KYNA) N-metil-D-aszpartát (NMDA)-receptorokon antagonista hatást fejt ki, így csökkenti a szabadgyök-képződés révén indukált neurotoxikus hatást, amely elsősorban a neocortexben, a striatumban és a hippocampusban alakul ki.

Ezek a régiók a neurodegeneratív betegségek (pl. Alzheimer-kór, Parkinsor-kór) predilekciós areái. A KYNA elő-anyaga, az L-kinurenin valamint bizonyos KYNA származékok átjutnak a vér-agy gáton. Ezen vegyületek hatékonyan képesek gátolni az agyi sérüléseket követő hiperexcitációt, ezáltal megfelelő koncentrációban neuroprotektív hatásúak, melyet különböző noxák okozta károsodás csökkentésében sikerült bizonyítani. Fontosak azok a kísérletes eredmények is, amelyek arra utalnak, hogy a kinureninek és metabolitjaik befolyásolják az agyi véráramlást: vazodilatációs hatásuk segítheti a neuroprotektív folyamatokat.

Kísérleteink célja az volt, hogy olyan reprodukálható, preklinikai állatmodelleket tervezzünk és alkalmazzunk, amelyek segítségével a különféle neurotoxikus ágensek által kiváltott károsodások kivédésére alkalmas összetevőket tesztelhetünk. Célul tűztük ki az ígéretesnek tűnő neuroprotektív anyagok tolerabilitásának és esetleges toxikus hatásainak meghatározását. Célunk volt bizonyos multidrug rezisztencia-asszociált fehérjék (MRP1, 2, 4 és 5) szerepének vizsgálata az MPTP által kiváltott neurotoxicitásban. Továbbá, hogy a KYNA amidok viselkedésre gyakorolt mellékhatásait vizsgáljuk meg C57B/6 egértörzsben. Célul tűztük ki az ionizáló sugárzás hatására kialakuló korai, és késői elváltozások összefüggéseinek viselkedésbeli, makro- és mikromorfológiai tanulmányozását, valamint a károsodás mechanizmusának befolyásolásával potenciális radio-neuroprotektív anyagok preklinikai vizsgálatát, melyek a későbbiekben alkalmasak lehetnek a klinikai gyakorlatban való kipróbálásra is.

C57B/6 egerekben az MPTP akut modellben történő alkalmazását megelőzően és azt követően egy héttel naponta intraperitonealisan alkalmazott szilimarin, naringenin, szulfinpirazon és allopurinol kezelést követően nagy teljesítményű folyadékkromatográfiával mértük a striatalis dopamin, 3,4-dihidroxifenilecetsav és homovanillinsav szinteket. A tesztelt MRP inhibítorok/stimulátorok közül egyik sem befolyásolta szignifikáns mértékben a dopamin és dopaminmetabolitok striatalis szintjét, azonban a naringenin kismértékben mérsékelte a dopaminszint csökkenését, míg az allopurinol nagymértékben fokozta az MPTP okozta letalitást. Ezen eredmények magyarázata egyrészt a toxikus anyagok glutation-konjugátumainak MRP1- és MRP2-mediálta transzportjának stimulálása által kiváltott jótékony hatás, másrészt az agyi urát, amely jelentős antioxidáns hatással rendelkezik, MRP4-mediálta effluxa miatt az oxidatív stressz fokozódása lehet.

Számos KYNA analóg tesztelése folyt, melynek segítségével egyre több adatunk lett ezen anyagok hatásáról. Nem tapasztaltuk markáns toxikus hatásukat egerekben sem.

Az általunk kialakított patkány rész-agy besugárzási technika humán sztereotaktikus BrainLab rendszerben, nagy pontosságú, egyszeri dózisleadást biztosít egyidejűleg két állat számára,

kifejezett agyi károsodást okozva az előre meghatározott térfogatban. Ezt követően kis volumenű rész-agy besugárzás történt 10 mm-es foton kollimátor kiöntése után 6 MeV energiájú elektron mezőkkel egyszerre 6 állaton. Két laterális opponáló mezővel kétoldali patkány hippocampus homogén besugárzását követő akut és krónikus hatások vizsgálatát végeztük. Ez a módszer jól alkalmazható a sugárhatás kísérletes tanulmányozására.

Az MR vizsgálat lehetővé tette az agyi strukturális károsodások megjelenésének noninvazív vizualizálását, és a besugárzási dózis–hatás vizsgálatát. Ennek alátámasztására szolgáltak a neurofunkcionális tesztek, majd végül a szövettani vizsgálatok. Eredményeink igazolják a fokális agyi besugárzást követő kognitív funkcióbeli, illetve szövettani szintű elváltozások kialakulását, valamint az L-alpha glycerylphosphorylcholine (GPC) kezelés fenti károsodásokra gyakorolt kedvező hatását.